



**MONTCLAIR STATE**  
UNIVERSITY

Montclair State University  
**Montclair State University Digital  
Commons**

---

Theses, Dissertations and Culminating Projects

---

5-2011

## Combining Bioinformatics and Chemical Biological Approaches to the Study of Signaling Pathways in Parasitic Nematodes

William R. De Martini  
*Montclair State University*

Follow this and additional works at: <https://digitalcommons.montclair.edu/etd>



Part of the [Bioinformatics Commons](#), [Biology Commons](#), and the [Chemistry Commons](#)

---

### Recommended Citation

De Martini, William R., "Combining Bioinformatics and Chemical Biological Approaches to the Study of Signaling Pathways in Parasitic Nematodes" (2011). *Theses, Dissertations and Culminating Projects*. 814. <https://digitalcommons.montclair.edu/etd/814>

This Thesis is brought to you for free and open access by Montclair State University Digital Commons. It has been accepted for inclusion in Theses, Dissertations and Culminating Projects by an authorized administrator of Montclair State University Digital Commons. For more information, please contact [digitalcommons@montclair.edu](mailto:digitalcommons@montclair.edu).

## **ABSTRACT:**

Lymphatic filariasis (elephantitis) is a disfiguring disease caused by thread-like nematodes. This disease affects the lives of over 120 million people and over one billion people are at risk for infection in endemic regions. Drugs used to treat this disease suffer from toxicity and emerging resistance and new therapies need to be identified. Our laboratory has been studying the filarial parasite, *Brugia malayi* (*B. malayi*), one of the causative agents of this disease. The laboratory is focused on the study of critical protein kinase signaling pathways, necessary for parasite protective anti-oxidative responses, as potential therapeutic targets. We have previously determined, using a bioinformatic and chemical biological approach that the *B. malayi* stress-activated protein kinase, Bm-MPK1, plays a critical role in defense against reactive oxygen species (ROS) stress generated by the innate immune system. The first part of my thesis extends our previous observation by examining the role of Bm-MPK1 in protection against reactive nitrogen species (RNS) which are also generated by the innate immune system during infection. I have found that treatment of the adult parasites with the Bm-MPK1 inhibitor, BIRB796, in the presence of RNS, leads to a reduction in parasite viability. These results implicate Bm-MPK1 in a protective signaling pathway against both ROS and RNS.

The second part of my thesis explores the generality of the use of bioinformatics, comparative genomics and chemical biological approaches for the identification of potential parasitic protein kinase targets. Using genomic data for the nematode *Caenorhabditis elegans* (*C.elegans*) and *B. malayi*, I have identified *B. malayi* Src kinase as a potential drug target. Treatment of adult *B. malayi* parasites with the clinically

approved human Src inhibitor dasatinib (Sprycel®), leads to decreased viability and defects in embryogenesis similar to those seen in *C. elegans* Src genetic knockdowns.

MONTCLAIR STATE UNIVERSITY

Combining bioinformatics and chemical biological approaches to the study of signaling pathways in parasitic nematodes

by

William R. De Martini

A Master's Thesis Submitted to the Faculty of

Montclair State University

In Partial Fulfillment of the Requirements

For the Degree of

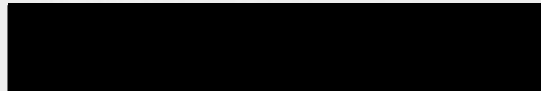
Master of Science

May 2011

College of Science and Mathematics

Department of Chemistry and Biochemistry

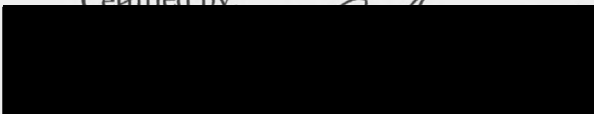
Thesis Committee:



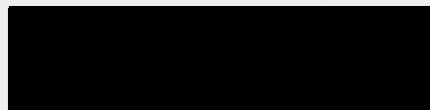
John Siekierka, PhD.

Thesis Sponsor

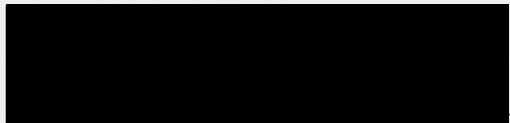
Certified by:



Robert Prezant, PhD  
Dean of College and Mathematics



Nina Goodey, PhD  
Committee Member



Elena Petroff, PhD  
Committee Member



Marc Kasner, PhD  
Department Chair

5/13/11

Date

**Combining bioinformatics and chemical biological approaches to the study of  
signaling pathways in parasitic nematodes**

A THESIS

Submitted in partial fulfillment of the requirements

For the degree of Masters of Science

by

William R. De Martini

Montclair State University

Montclair, NJ

2011

## Acknowledgements

I thank foremost Dr. John Siekierka for accepting me in his research laboratory and being my thesis advisor/mentor for the last one and half years. Dr. Siekierka's knowledge and experience in the field has benefited my graduate education more than I could have expected.

I thank Dr. Ronald Goldberg for all of the training and advice he has given me in numerous laboratory experiments. He has shared his extensive experience in laboratory research which has made me a better scientist.

I thank Dr. Nina Goodey and Dr. Elena Petroff for accepting to be in my thesis review committee members. I would like to give Dr. Petroff additional gratitude for allowing me to use her laboratory facilities.

I thank my laboratory colleagues Akriti Patel, Agnieszka Chojnowski, Katie Gaskill, and James Luginsland for all their help in my research studies for this thesis.

I thank my family and friends for all of their moral support.

Lastly, I would like to thank the Department of Chemistry and Biochemistry and the Sokol Institute for Pharmaceutical Life Sciences.

## TABLE OF CONTENTS

ABSTRACT.....	I
THESIS SIGNATURE.....	III
TITLE PAGE.....	IV
ACKNOWLEDGEMENTS.....	V
LIST OF FIGURES.....	VIII
LIST OF TABLES.....	X
INTRODUCTION:.....	1
I. <i>Lymphatic Filariasis</i> .....	1
II. <i>Filarial Parasites and Oxidative Stress</i> .....	3
<i>The p38-stress activated protein kinase family</i> .....	3
<i>PMK-1 and Bm-MPK1 MAPKs and oxidative stress</i> .....	5
<i>The role of nitric oxide and peroxynitrite in oxidative stress</i> .....	6
III. <i>Application of Bioinformatics and Chemical Biology to filarial parasite drug target discovery</i> .....	7
MATERIALS AND METHODS.....	9
<i>Immobilized Metal Affinity Ion Polarization Assay (IMAP)</i> .....	9
<i>Motility of B. malayi Adult Parasites</i> .....	10
<i>SDS Page/Western Blotting of active Bm-MPK1 RNS-induced stress</i> .....	11
<i>Screening of Kinase Inhibitors against B. malayi based on the C. elegans kinome</i> .....	12
<i>Evaluation of Dasatinib on B. malayi parasites</i> .....	12
RESULTS.....	13
<i>p38 inhibitor evaluations against Bm-MPK1</i> .....	13
<i>Effect of BIRB796 on RNS-induced stress in Adult B. malayi Parasites</i> .....	13
<i>Activation of Bm-MPK1 by SIN-1 and inhibition by BIRB796</i> .....	14
<i>Bioinformatic analysis of the B. malayi and C. elegans kinomes. Use of the src kinase inhibitor dasatinib as a chemical probe</i> .....	14
DISCUSSION.....	16
<i>Bm-MPK1 and its role in RNS-induced stress</i> .....	16

<i>Drug Target Discovery: Use of Bioinformatics and Comparative Genomics with Chemical Biological Approaches to study Parasite Protein Kinase Signaling Pathways</i> .....	17
FIGURES.....	19
TABLES.....	29
REFERENCES.....	39
APPENDIX: The role of a <i>Brugia malayi</i> p38 MAP kinase ortholog (Bm-MPK1) in parasite anti-oxidative stress responses	



## List of Figures

Figure 1. The life cycle of the filarial nematode <i>B. malayi</i> .....	19
Figure 2. Structure of the competitive inhibitor SB203580.....	20
Figure 3. Structure of the allosteric p38 inhibitor BIRB796.....	20
Figure 4. The synthesis of NO from L-Arginine.....	20
Figure 5. The structure of SIN-1 and its auto-oxidation for the production of NO and O <sub>2</sub> <sup>-</sup> .....	21
Figure 6. Dose response curves of BIRB796, SB202190 and VX702 against Bm-MPK-1.....	21
Figure 7. Percent control of motility with RNS-induced stress on female adult <i>B. malayi</i> within 48 h .....	22
Figure 8. <i>In vivo</i> activation and inhibition of Bm-MPK1.....	23
Figure 9. The kinomes of <i>C. elegans</i> and <i>B. malayi</i> share 141 kinases.....	24
Figure 10. Conformational differences in the 10 μM dasatinib treatment group.....	24
Figure 11. Effects of dasatinib on adult female <i>B. malayi</i> motility.....	25

Figure 12. The dispersion of microfilaria, premicrofilaria and early stage embryos  
in the control 0.1% DMSO group.....26

Figure 13. The dispersion of microfilaria, premicrofilaria and early stage embryos  
in the 10  $\mu$ M dasatinib treatment group.....27

Figure 14. The phenotypical effects of 10  $\mu$ M dasatinib on early stage embryos  
in *B. malayi*.....28

## List of Tables

Table 1. IC <sub>50</sub> values of p38 inhibitors against p38 and Bm-MPK1 .....	26
Table 2. Crude extracts recovered from adult <i>B. malayi</i> parasites.....	26
Table 3. Seventy-seven kinases that are orthologous in <i>C. elegans</i> , <i>B. malayi</i> and Humans.....	27

## INTRODUCTION:

### I. Lymphatic Filariasis

Lymphatic filariasis (elephantitis) is a disfiguring disease caused by the thread-like nematodes *Brugia malayi*, *Brugia timori* and *Wuchereria bancrofti*. This disease affects the lives of over 120 million people and over one billion people are at risk for infection [1, 2]. The majority of lymphatic filariasis is caused by *W. bancrofti* and is prevalent in the tropics. *B. malayi* is found in South Asia and *B. timori* in Timor and the Flores areas of Indonesia [1]. Unlike *W. bancrofti* and *B. timori*, *B. malayi* can infect mammals such as gerbils and cats providing an animal model for the disease.

In this disfiguring disease, the human plays the role as the host and the mosquito, *Mansonia spp*, the vector. Upon taking a blood meal, the mosquito picks up microfilaria, the immature stage of the parasite, present in the human host. These ingested microfilaria mature to the third stage larvae form (L3) and migrate to the head and proboscis of the mosquito. During the next blood meal, the L3 larva are transmitted into the human host and travel to the efferent lymphatics and subcapsular sinus. The parasite will mature to the adult stage within 6 to 12 months. Females will produce microfilariae after mating males, completing the life cycle of this organism.

Microfilariae in an infected human can be detected within 41 to 46 weeks post infection. Adult parasites have a life span of several years within the host [3] (Figure 1).

Current treatment for lymphatic filariasis is targeted against the microfilaria. A popular macrocyclic lactone, ivermectin (Mectizan®), is used to treat lymphatic filariasis. It has been shown that ivermectin inhibits L3 molting and reduce microfilariae output by

sterilizing the female adults [4]. Ivermectin targets the glutamate-gated  $\text{Cl}^-$  and  $\text{K}^+$  channels of nematodes which causes paralysis of the body wall muscle, including the pharynx [1]. Another drug, diethylcarbamazine (DEC), dramatically reduces microfilarial count in the blood within a few minutes. In rodent models, it has been demonstrated that DEC acts on microfilariae by unmasking antigenic determinates that facilitate killing of the organism by kupffer cells of the reticuloendothelial system [4]. It has also been found that inducible nitric oxide is essential for DEC activity against microfilaria [5]. DEC was the most popular drug to treat the disease, however the microfilaricidal ivermectin has been shown to have fewer side effects [6]. A third drug, albendazol, considered an effective and safe drug for treating intestinal helminthes, is commonly co-administered with either ivermectin or DEC. It has been proven to have long-term effectiveness in decreasing microfilaria in *W. bancrofti* infections. However, there is insufficient evidence that co-administration of albendazol with ivermectin and DEC provides any advantage over these drugs alone [1]. New drugs are needed due to emerging issues with toxicity and resistance with currently used drugs. [7, 8].

Our laboratory has been focused on parasitic protein kinases as potential drug targets. We have previously determined that a parasitic ortholog, Bm-MPK1, of human p38 mitogen activated protein kinase (p38) and *C. elegans* PMK-1 protein kinase is required for parasite protective responses against oxidative stress [9]. My thesis research extends this work to include stress due to reactive nitrogen species (RNS). In addition, using a comparative genomics and chemical biological approach, I have identified a *B. malayi* Src tyrosine kinase as a potential drug target.

## II. Filarial Parasites and Oxidative Stress

Resistance of filarial nematodes to oxidative stress is essential to long term survival inside the human host. These parasites must protect themselves from host innate immune responses which produce reactive oxygen and nitrogen species such as superoxide and nitric oxide. Filarial parasites have a number of mechanisms which protect the parasite against oxidative stress [10, 11]. One important mechanism has been identified in our laboratory. Our lab has identified a *B. malayi* protein kinase, Bm-MPK1, which plays a crucial role in protection against oxidative stress [9]. Interestingly, Bm-MPK1 is an ortholog of the human p38 stress-activated mitogen-activated protein kinase family.

### *The p38-stress activated protein kinase family*

Mammalian cells respond to stress such as UV, inflammatory and oxidative stress through the activation of stress activated protein kinases. There are two families of stress-activated protein kinases, the C-terminal JUN kinases (JNK), and the p38 mitogen-activated protein kinase family. A stress stimulus from the environment leads to the activation of a protein kinase cascade initiated by a mitogen activated kinase kinase kinase (MKKK), which in turn phosphorylates a mitogen activated kinase kinase (MKK). MKK dually phosphorylates JNK and p38 on a conserved T-X-Y motif leading to activation of JNK and p38 which in turn, produces a biological response. [12]. This thesis will focus on the p38 MAPK family and its relationship to Bm-MPK1.

The p38 MAPK family consists of the four isoforms, p38 $\alpha$ , p38 $\beta$ , p38 $\gamma$ , and p38 $\delta$  which share 60% homology overall. The p38 $\alpha$  and p38 $\beta$  isoforms share 75% homology overall [13]. It has been observed that p38 $\alpha$  is the predominant form in monocytes and

macrophages [14], p38 $\gamma$  is most significantly expressed in skeletal muscle and p38 $\delta$  is found mostly in the testis, pancreas, kidney and small intestine [13]. Human p38 $\alpha$  and  $\beta$  was originally identified as the molecular target of the pyridinyl class of compounds that were shown to inhibit the biosynthesis of inflammatory cytokines such as tumor necrosis factor (TNF) in lipopolysaccharide (LPS)- stimulated human monocytes [15].

Activation of p38 is shown to occur in response to T cell antigen receptor (TCR) signaling and participates in thymocyte development, differentiation of T helper type 1 cells and activation of mature T cells in response to antigen. In addition to the activation of the p38 family in response to stress such as hyperosmolarity, UV irradiation and heat shock p38 signaling is also important for cell survival, apoptosis and induction of cytokine genes. Activation of p38 occurs by dual phosphorylation of Thr-180 and Try-182 in a TGY motif by MKK3/6, and MKK4 in some cases [12]. The TGY motif is located within a regulatory loop between subdomains VII and VIII. As a result of phosphorylation, a conformational change occurs which enables ATP and substrate to bind the kinase. The duration of phosphorylated p38 is controlled by phosphatases such as protein phosphatase 1, protein phosphatase 2A or MAPK phosphatase [16]. Substrates for active p38 include transcription factors ATF2, Elk-1 and SAP1 and kinases MAPKAP-K2 and MAPKAP-K3 [13].

In view of the therapeutic importance of p38 (i.e. in inflammation and oncology) numerous programs have been established to identify selective and potent inhibitors of p38. One of the first inhibitors developed is the prototypic pyridylimidazole SB203580 is a competitive inhibitor of p38 (Figure 2). SB203580 has been used as a template for a vast majority of p38 inhibitors [14]. This compound inhibits of the p38 $\alpha$  and p38 $\beta$

isoforms, but not the p38 $\gamma$  or p38 $\delta$ . SB203580 prevents ATP binding through the interaction of its fluorine atom with Thr106 of the kinase. The drug is oriented with His107 and Leu108 of the ATP pocket [13]. Inhibitors such as SB202190 and VX702 are also competitive for the ATP substrate.

Novel classes of allosteric inhibitors have recently been developed. BIRB796 is an allosteric diaryl urea inhibitor that can bind to all four isoforms (Figure 3). This compound binds with a slow on rate to p38 to a site spatially distinct from the ATP pocket. A conformational change occurs on a highly conserved DFG motif upon binding of BIRB796 which prevents ATP binding to its designated pocket. The apparent IC<sub>50</sub> of BIRB796 against p38 decreases with incubation time with kinase and inhibitor, with an IC<sub>50</sub> of 98 nM at 0 h and 8 nM at 2 h [17].

### ***PMK-1 and Bm-MPK1 MAPKs and oxidative stress***

The roundworm *C. elegans* is a powerful model system for the study of numerous biological systems. Its genome has been sequenced and annotated and can be accessed at [www.wormbase.org](http://www.wormbase.org). The *C. elegans* stressed-activated protein kinase, PMK-1 is an ortholog of human p38 [9]. It has been determined through genetic means, that PMK-1 is essential for innate immunity and protection against oxidative stress in *C. elegans*. [18-20] PMK-1 phosphorylates and activates the transcription factor SKN-1 leading to the induction of phase II detoxification gene expression [19]. We have found that PMK-1 is an ortholog of the *B. malayi* kinase Bm-MPK1 mentioned previously. Using a chemical biological approach, we demonstrated that inhibitors of human p38 inhibit the activity of



Bm-MPK1 leading to the inability of parasites to respond to oxidative stress compromising parasite viability [9].

### *The role of nitric oxide and peroxynitrite in oxidative stress*

In addition to ROS, the generation of reactive nitrogen species (RNS) such as nitric oxide are produced by the innate immune system. Nitric oxide (NO) plays an important role in human biology. Free NO is a small molecule radical ( $t_{1/2} = \sim 5$  seconds [21]) that can easily permeate cell membranes. At low concentrations, it is known to be a vasodilator and results in an increase in the flow of blood through vessels by smooth muscle relaxation. NO is produced by the enzymatic activity of nitric oxide synthase (NOS) which oxidizes the guanidine group of L-arginine (Figure 4). The reaction requires the cofactor tetrahydrobiopterin,  $BH_4$ , and the additional reactants  $O_2$  and NADPH. High levels of nitric oxide are generated during inflammation and can modify and damage DNA, RNA, lipids and proteins [22]. There are three known isoforms of NOS; neuronal (nNOS), epithelial (eNOS) and inducible (iNOS). Macrophages possess the iNOS isoforms and generate NO as part of their biochemical defense against foreign pathogens [23].

Peroxynitrite is a damaging reactive nitrogen species (RNS) that is produced by the interaction of NO with superoxide ( $O_2^{\cdot-}$ ). It is a short lived compound that has a higher permeability than superoxide. Peroxynitrite has the ability to inhibit Mn superoxide dismutase by nitration of a critical Tyr-34 residue. This allows an increase in the amount of superoxide and hydrogen peroxide which increases damage to mitochondria.

Peroxynitrite produces the following cytotoxic effects: initiation of lipid peroxidation,

direct inhibition of mitochondrial respiratory chain enzymes, inactivation of membrane sodium channels, inactivation of glyceraldehydes-3-phosphate dehydrogenase, and inhibition of membrane  $\text{Na}^+/\text{K}^+$  ATP-ase activity. [24].

The role of the *B. malayi* stress-activated protein kinase, Bm-MPK1, in RNS has not been evaluated. In order to study the effects of RNS-induced stress, the compound linsidomine chlorhydrate (SIN-1) was used to mimic this stress. SIN-1 undergoes auto-oxidation to produce NO and  $\text{O}_2^{\cdot-}$  (Figure 5), which subsequently lead to the formation of peroxynitrite. The first part of this thesis will evaluate the role of Bm-MPK1 in anti-RNS stress.

### **III. Application of Bioinformatics and Chemical Biology to filarial parasite drug target discovery**

Protein kinases are one of the largest and most important of the protein families accounting for ~2% of the genes in a variety of eukaryotic genomes. Protein kinases are important therapeutic targets [25]. The Bcr/Abl kinase inhibitor imatinib (Gleevec®), is the first targeted cancer therapy used clinically to treat chronic myelogenous leukemia and gastrointestinal stromal tumors. Kinases phosphorylate other proteins in the cell, which modifies the activity, location and the affinities of nearly 30% of all cellular proteins at any given time. They direct signal transduction and coordination of complex pathways, many of which are highly conserved between different species.

Bioinformatics and comparative genomics have been shown to be powerful tools in analyzing the evolutionarily conserved function of kinases. Nematodes share 153 kinase subfamilies with humans, and provide orthologs for 81% (419/518) of all human kinases.

Some of these human orthologs have selective synthetic inhibitors which can potentially be used to elucidate signaling pathways in nematodes [26].

The NIAID/NIH Filariasis Research Reagent Resource Center (FR3) provides a database on their website that correlates *C. elegans* genes with putative *B. malayi* homologs. A total of 4,620 *C. elegans* genes having *B. malayi* orthologs are listed, of these, 2,547 orthologs are listed having the corresponding *C. elegans* RNAi knockdown phenotypes. A database of the *C. elegans* kinome ([www.kinase.com](http://www.kinase.com)) lists 438 protein kinase genes. The *B. malayi* kinome contains 225 kinase genes [27]. Using this database and the FR3 database allows a comparison of protein kinase orthologs between *C. elegans* and *B. malayi* along with RNAi phenotypic annotation. The use of RNAi on the adult *B. malayi* parasite has met with very little success largely due to the absence of genes in the parasite required for RNA uptake and distribution [28, 29]. One approach to potentially overcome this limitation to studying protein kinase function (i.e. through RNAi knockdowns) is to compare protein kinase orthologs between *C. elegans* and *B. malayi* and identify those kinases exhibiting a critical phenotype and for which specific inhibitors against human orthologs exist. It may therefore be possible to examine the effects of treating *B. malayi* parasites with specific inhibitors and comparing the resulting phenotypes with the *C. elegans* RNAi knockdowns. Presented in this thesis are the results of using a commercially available Src tyrosine protein kinase inhibitor to compare the phenotypes between inhibitor treated parasites and the corresponding *C. elegans* RNAi knockdown.

## MATERIALS AND METHODS

### *Immobilized Metal Affinity Ion Polarization Assay (IMAP)*

The following compounds were previously assayed for potency against Bm-MPK1 in the lab: BIRB796 (Axon Groningen, Netherlands), SB203580 (Selleck, Houston, TX), RWJ67657 (Dr. Fina Liotta, Montclair State University). Additional p38 inhibitors SB202190 (BIOMOL/Enzo Farmingdale, NY) and VX702 (Selleck) were assayed against Bm-MPK1 for this thesis. All inhibitors were first dissolved in dimethyl sulfoxide (DMSO) at a 10 mM concentration. Inhibitors were assayed for potency using an IMAP assay (Molecular Devices; Sunnyvale, California). IMAP is a high-throughput fluorescent based assay suitable for high-throughput screening. A kinase reaction was performed by adding enzyme, a fluorescent substrate (peptide) and ATP for an incubation of 1 h. The reaction was terminated by the addition of a nanoparticle suspension containing a coupled trivalent metal ion ( $M^{III}$ ) which binds to the phosphorylated peptide product. The binding of the metal ion to the phosphorylated fluorescent substrate generated molecules with a slower rotational speed and thus increased the Fluorescence polarization (FP) signal [30].

Active Bm-MPK1 was generated as described in our recently published paper [9]. The IMAP assay was conducted as per manufacturer's instructions (Molecular Devices). Activated Bm-MPK1, inhibitor and the fluorescent peptide, FAM-p38tide (Molecular Devices) were prepared in 1 mM dithiothreitol (DTT) (Fisher Scientific), 100  $\mu$ M ATP (Sigma-Aldrich), 1X Reaction Buffer-Tween (10 mM Tris-HCl pH 7.2, 10 mM  $MgCl_2$ , 0.05%  $NaN_3$  and 0.01% Tween-20) buffer (Molecular Devices). Inhibitor concentrations

were serially diluted starting from 10,000 nM to 14 nM. The kinase reaction was initiated by using 60 ng of active Bm-MPK1, 100 nM fluorescent substrate and inhibitor which was allowed to incubate at room temperature for 1 h on a plate shaker (Barnstead/Lab-line). All kinase reactions were performed at a volume of 20  $\mu$ L in a low volume black 96-well plate (Corning Lowell, MA). After the 1 hour incubation, the reaction was terminated with the addition of 60  $\mu$ L of PBB containing the nanoparticles (1:600) prepared as per manufacturer's instructions (Molecular Devices). An additional incubation period of 1 h was performed and the plate was read using Synergy 2 microplate reader. The plate was read using an excitation wavelength of 485 nm and an emission wavelength of 528 nm [30]. The plate consisted of background containing substrate and ATP and a max with Bm-MPK1, peptide and ATP. The data was analyzed in Microsoft Excel, and was corrected for background.  $IC_{50}$  values were calculated based on a four parametric logistic fit in Microsoft Excel using Solver.

#### *Motility of B. malayi Adult Parasites*

Female adult *B. malayi* parasites were procured from the NIAID/NIH Filariasis Research Reagent Resource Center (FR3) at the University of Georgia. Parasites were placed on 24 well plates (BD Franklin Lakes, NJ) in 2 mL of complete media and allowed to rest for 24 h. Media consisted of Advanced RPMI 1640 (Invitrogen, Carlsbad, CA) supplemented with 25 mM HEPES, L-Glutamine, Penicillin-Streptomycin (Invitrogen), Amphotericin B solution (Invitrogen), 5% heat inactivated fetal bovine serum (FBS) (Invitrogen). Adult parasites were then cultured in complete media supplemented with the desired concentrations of SIN-1 (Invitrogen), dasatinib (ChemieTek; Indianapolis, Indiana) or BIRB796 (Axon). Motility of each adult was examined every 24 hours.

Parasite motility was given a score from 0 to 4 with: 4, rapid movement and largely coiled; 3, moderate movement and uncoiled; 2, slow movement and uncoiled; 1, twitching movement and uncoiled; 0, no motility (dead).

*SDS Page/Western Blotting of active Bm-MPK1 RNS-induced stress*

The effect of RNS-induced stress was examined by Western blotting probing against pTGpY. Six adult worms were used per treatment group. The combination of SIN-1 and BIRB796 was pretreated with BIRB796 for 1 h. After 1 h of exposure, extracts of the adults were made by mortar and pestle in a solution containing M-PER (Thermo Scientific) with phosphatase inhibitor (10 mM sodium fluoride, 2 mM pyrophosphate, 2 mM Beta-glycerol phosphate and 5 g/ml). Protein content was measured by Bradford assay (Sigma-Aldrich; St. Louis, MO, ) [31] with BSA as the standard. Twenty-six micrograms of protein from each treatment was loaded on to an SDS-PAGE (Table 2). Samples of each treatment group were prepared in NuPAGE SDS sample buffer (Invitrogen) containing DTT and placed in a heating block at 90°C for 5 minutes. The samples were loaded on a 10-well NuPAGE 4-12% Bis-Tris 1.0 mm gel (Invitrogen) and were run at 200 V for 40 minutes using MOPS SDS running buffer (Invitrogen). Novex sharp pre-stained protein standards (Invitrogen) were loaded on the gel as molecular weight markers. The gel was transferred onto a PVDF membrane, previously soaked in methanol for 30 sec, using NuPAGE® Transfer Buffer (Invitrogen) containing 10% methanol and 0.25% SDS using a TE77XP Semi-DryBlotter (Hoefer Holliston, MA) for 1 h at 54 mA. The membrane was incubated with rabbit Anti-Active® (pTGpY) affinity purified polyclonal IgG antibody 1:2000 (Promega, Madison, WI) for 1 h and incubated with alkaline phosphatase (AP)-linked secondary antibody 1:30,000 anti-rabbit (Sigma-

Aldrich). Chromogenic Western Blue® Stabilized Substrate for AP (Promega) was added to the membrane for the elucidation of active, phosphorylated Bm-MPK1 bands.

Densitometry was analyzed using Image-J program [32].

#### *Screening of Kinase Inhibitors against B. malayi based on the C. elegans kinome*

Data was downloaded from the databases from both the FR3 website

(<http://www.filariasiscenter.org>) and Kinase.com ([www.kinase.com](http://www.kinase.com)) regarding *C. elegans*

RNAi knockdowns and their corresponding kinases. A query was performed through

Microsoft Access on the two databases that matched the corresponding genes from the *C.*

*elegans* RNAi knockdowns data with the corresponding *B. malayi* orthologs that translate

protein kinases. This was performed by creating a table for each database and linking

each table by the *C. elegans* ortholog accession number.

#### *Evaluation of Dasatinib on B. malayi parasites*

Screening of the kinase inhibitor on the *B. malayi* parasite was performed similarly as

stated in the section *Motility of B. malayi Adult Parasites*. Parasites were transferred into

fresh media every 48 h. Parasite secretions of microfilaria were monitored every 24 h

during the course of the experiment.

## RESULTS

### *p38 inhibitor evaluations against Bm-MPK1*

Several commercially available p38 inhibitors were previously tested against p38 and Bm-MPK1. I evaluated an additional two new inhibitors, SB202190 and VX702. The IC<sub>50</sub> values for SB202190 and VX702 were determined to be 220 and 4,270 nM respectively as determined by two separate assays. Interestingly, VX702 is a potent inhibitor of human p38 exhibiting an IC<sub>50</sub> of 4.0 nM, 1068 times less potent against Bm-MPK1. This suggests that the inhibitor binding site differs significantly between humans and *B. malayi* potentially allowing the design of more selective Bm-MPK1 inhibitors. Based on its potency and prior use studying ROS-induced stress, I used BIRB796 to evaluate the role of Bm-MPK1 in RNS-induced stress (Figure 6, Table 1).

### *Effect of BIRB796 on RNS-induced stress in Adult B. malayi Parasites*

A titration of SIN-1 indicated that 0.250 mM is the optimal concentration to perform RNS-induced stress experiments without any overt effects on parasite viability. Similarly, we have previously observed that using 10 µM BIRB796 with the parasites does not affect viability [9]. Upon treatment of parasites with the combination of 0.250 mM SIN-1 and 10 µM BIRB796, parasite motility was significantly reduced at 24 h (25% of control) and 48 h (50% of control) (Figure 7). Decreases in the motility of parasites correspond to decreased viability [33].



### *Activation of Bm-MPK1 by SIN-1 and inhibition by BIRB796*

Bm-MPK1 was activated *in vivo* under conditions of RNS-induced stress. Western blotting of adult worm extracts exposed to 0.250 mM SIN-1 for 1 hour revealed a band at ~42 kDa when probed with anti phosphor p38 ( pTGpY) antibodies. These antibodies only bind to the phosphorylated form of Bm-MPK1. A 4 fold increase in phosphorylated Bm-MPK1 was observed when compared to control. An approximate 50% reduction in activated Bm-MPK1 was observed upon the addition of 10  $\mu$ M BIRB796 when compared to 0.250 mM SIN-1 alone (Figure 8 A, B). These experiments demonstrate activation of Bm-MPK1 within the parasite upon SIN-1 treatment and subsequent inhibition in the presence of the p38 inhibitor BIRB796.

### *Bioinformatic analysis of the B. malayi and C. elegans kinomes. Use of the src kinase inhibitor dasatinib as a chemical probe.*

A total of 435 kinases are present in *C. elegans*, whereas approximately half this number, 225 are present in *B. malayi* (Figure 9) [27]. A query performed using Microsoft Access provided a list of 77 *C. elegans* protein kinases serving critical functions (as determined using RNAi knockdown technology) having orthologs in *B. malayi*. (Figure 10, Table 3). Twelve of these kinases have commercially available inhibitors. It was decided to focus on src kinase since RNAi knockdowns in *C. elegans* exhibited severe defects in embryogenesis and locomotion. In addition, a selective src inhibitor, dasatinib, is commercially available as a chemical probe.

Treatment of parasites with 10  $\mu$ M dasatinib induced severe locomotion defects within three hours. All treated parasites curled up into a corkscrew like conformation as

opposed to the normal extended conformation (Figure 10 A, B). These parasites returned to their previous extended confirmation when examined at 24 h, but exhibited a 50% reduction in motility compared to the control group (Figure 11). No effects were observed with 1  $\mu$ M dasatinib. Further evaluation was not possible beyond 72 hours due to a reduction in control group motility. It was observed that the secretion of microfilaria was significantly reduced with 10  $\mu$ M dasatinib treatment in the first 24 hours onward compared to the control group. By 96 h, virtually no secretion was observed. Dissection of control group parasites revealed relatively equal distribution of microfilaria, premicrofilaria and early stage embryos (Figure 12), whereas a dissection of adult parasites exposed to 10  $\mu$ M dasatinib for 96 h had a distribution of mostly early stage embryos and premicrofilaria (Figure 13). Additionally, early stage embryos from the 10  $\mu$ M dasatinib group appeared morphologically abnormal when compared to the control group (Figure 14 A, B).

## DISCUSSION

### *Bm-MPK1 and its role in RNS-induced stress*

A common finding in both protozoan and helminthic infections is the production of NO by cells of the innate immune system. Elevation of NO has been confirmed in human patients infected with *B. malayi*. It is believed NO is produced through the induction of iNOS in the direct response of the host's innate immune system to the parasite antigens or possibly due the endotoxin derived from the endosymbiotic bacteria, *Wolbachia*, present in the nematode [34]. In this thesis, I have demonstrated that the *B. malayi* p38 ortholog, Bm-MPK1, is sensitive to the effects of RNS induced stress through the use of the NO donor SIN-1. At sub-optimal, no-effect doses of SIN-1 (0.250 mM), treatment of parasites with the Bm-MPK1 inhibitor, BIRB796, renders the parasites sensitive to RNS leading to a significant reduction in motility and viability within 24-48 h of treatment. These results show that RNS, like ROS, leads to activation of Bm-MPK1 as part of an anti-stress response. Inhibition of Bm-MPK1 with BIRB796 leads to an increased susceptibility of the parasite to the effects of RNS and ROS and compromises viability. RNS stress has been shown to lead to the activation of p38 in mammalian cells as part of an anti-stress response [35, 36]. Similarly, I have shown in this thesis that Bm-MPK1 is activated 4- fold in parasites treated with 0.250 mM SIN-1 and is inhibited by 50% with the addition of 10  $\mu$ M BIRB796.

*Drug Target Discovery: Use of Bioinformatics and Comparative Genomics with Chemical Biological Approaches to study Parasite Protein Kinase Signaling Pathways*

The study of filarial parasite biology and biochemistry suffers from a lack of genetic techniques to study gene function. As mentioned previously, techniques such as RNAi knockdowns which offer a powerful tool in studying *C. elegans* biology, have met with poor results in filarial nematodes. To circumvent this problem, we have been combining bioinformatics and chemical biological approaches to study protein kinase signal pathways in *B. malayi*. A successful example of this approach can be found in our recent research with the *B. malayi* stress-activated protein kinase Bm-MPK1. This kinase was identified as a human p38 and *C. elegans* PMK-1 ortholog through database blast searches. Examining the results of PMK-1 knockdown studies in WormBase, it was found that PMK-1 is required for *C. elegans* innate immunity and protection against arsenate-induced oxidative stress [18-20]. Using selective p38 inhibitors, we demonstrated that inhibition of Bm-MPK1 with the allosteric inhibitor, BIRB796, leaves *B. malayi* susceptible to arsenate-induced stress in a manner similar to that observed in *C. elegans* RNAi knockdowns of PMK-1 [9].

To further extend the generality of this approach, I identified 77 proteins kinases with critical functions in *C. elegans* that have orthologs in *B. malayi*. Twelve of these kinases have commercially available inhibitors, which includes the p38 ortholog Bm-MPK1. I choose the *B. malayi* src protein kinase as a target and used the human src inhibitor dasatinib, as a chemical biological probe to study the function of *B. malayi* src. Dasatinib, at a concentration of 10  $\mu$ M, produced defects in viability, embryogenesis and microfilaria secretion in the adult *B. malayi* parasite. These phenotypes mirror those

reported using RNAi knockdown approaches for the *src-1* gene in *C. elegans* which include defects in embryogenesis and locomotion.

In summary, I have shown that combining bioinformatics and chemical biology can be a useful tool for studying protein kinase function in the parasitic nematode *B. malayi*.

Through the use of selective kinase inhibitors, the phenotypes observed in *C. elegans* RNAi knockdown studies can be recapitulated with synthetic inhibitors in *B. malayi*. The use of selective, small molecule, inhibitors to study other parasitic protein functions, e.g. metalloproteinases, GPCRs, *etc.* warrants consideration.

FIGURES

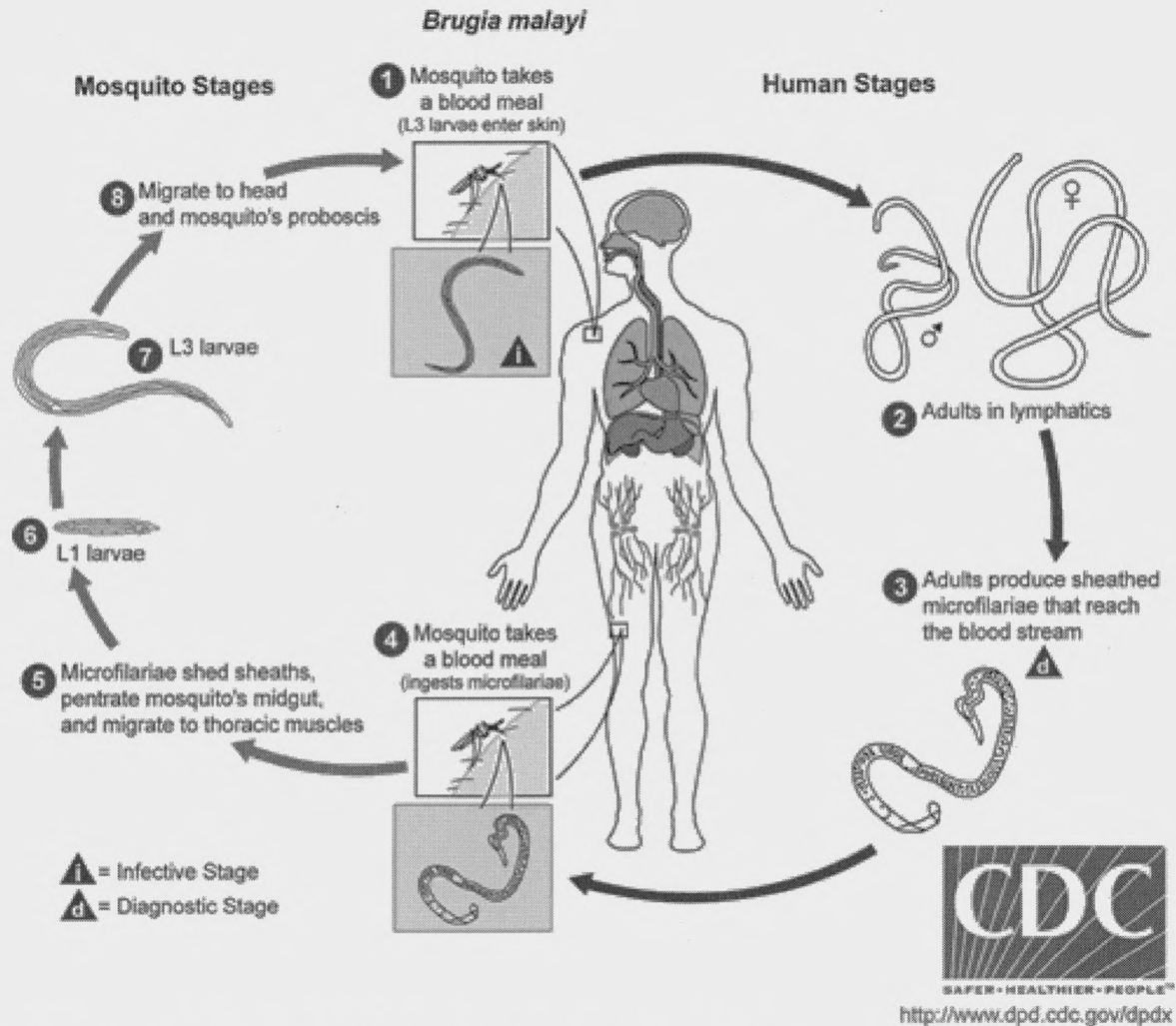


**Figure 1. The life cycle of the filarial nematode *B. malayi***

The *B. malayi* parasite uses the mosquito *Mansonia spp.* as a vector to invade the human host. An infected mosquito will inject the third stage larval form of the parasite up blood feeding. The L3 will progress to the adult stage in the lymphatic system of the human. Upon mating, females will produce the immature larval stage, the microfilariae, and secrete them into the blood stream of the human during night time. An uninfected mosquito will ingest the microfilaria during a blood feeding, where the infectious L3 larva form will develop and continue the cycle of infection.

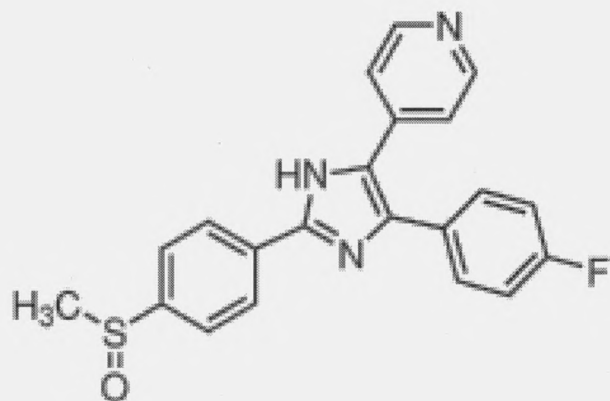


Figure 2. Structure of the competitive inhibitor SB203580 (Sigma).

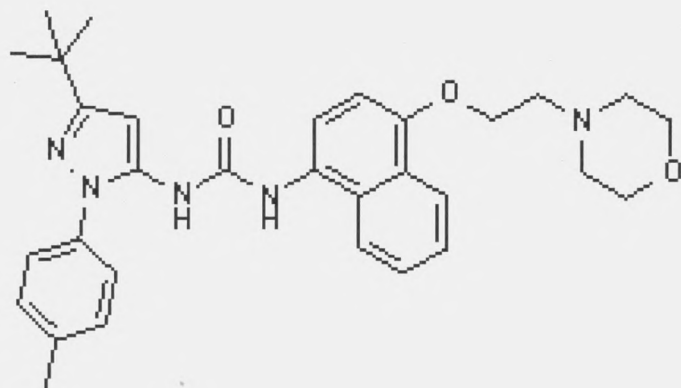


Figure 3. Structure of the allosteric p38 inhibitor BIRB796 (Axon).

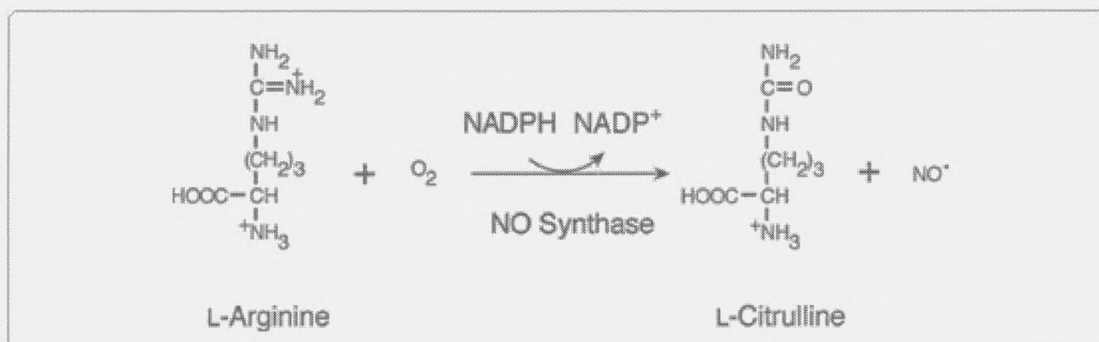


Figure 4. The synthesis of NO from L-Arginine ([www.invitrogen.com](http://www.invitrogen.com)).

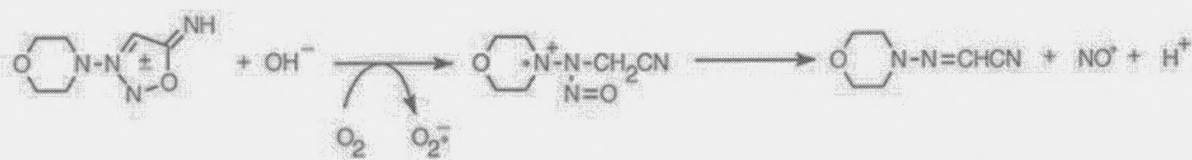


Figure 5. The structure of SIN-1 and its auto-oxidation for the production of NO and  $O_2^{\cdot-}$  (www.invitrogen.com).

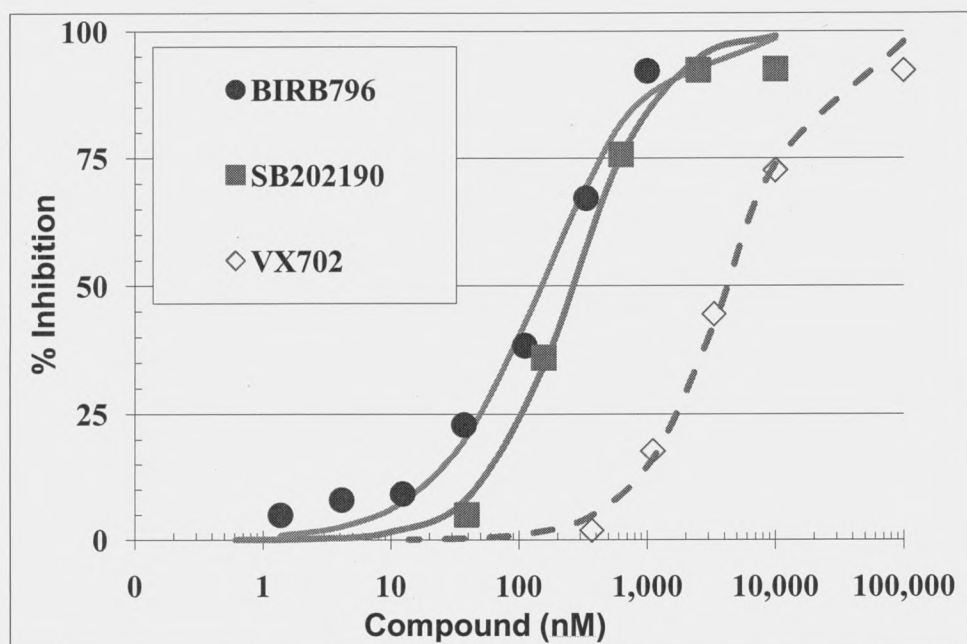
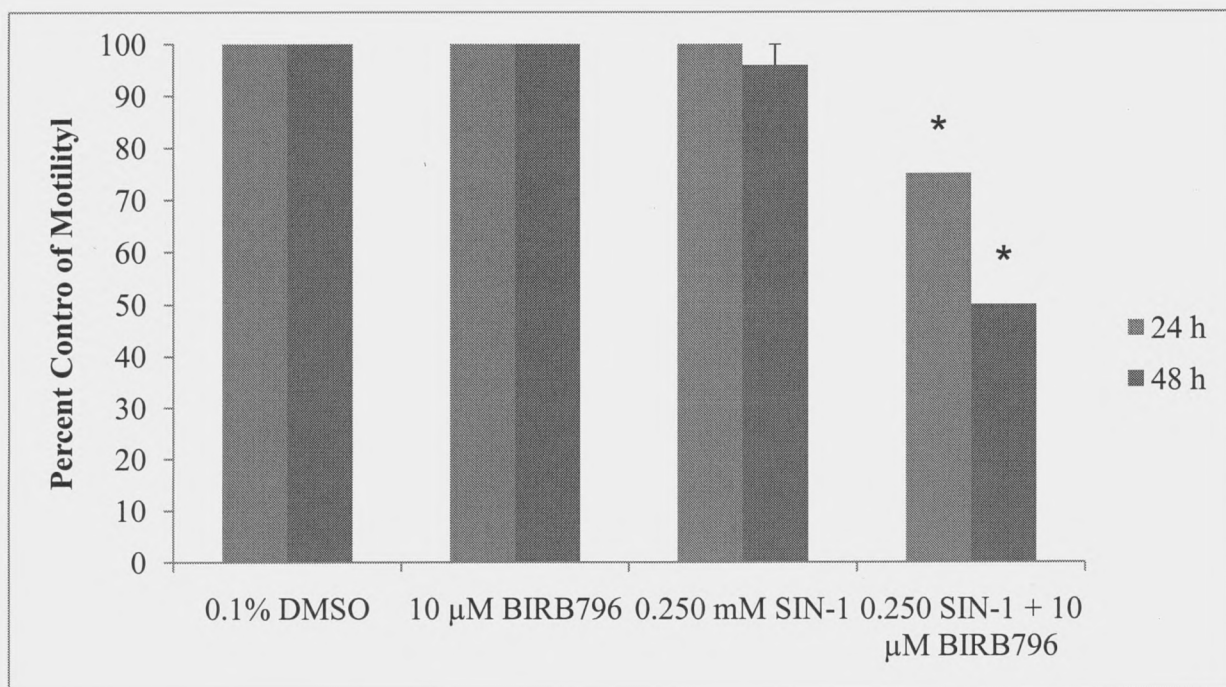


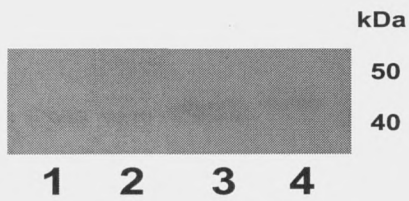
Figure 6. Dose response curves of BIRB796, SB202190 and VX702 against Bm-MPK1. The  $IC_{50}$  values of BIRB796, SB202190 and VX702 are 152, 220 and 4,270 nM respectively.





**Figure 7. Percent control of motility with RNS-induced stress on female adult *B. malayi* within 48 h.** The data was evaluated as % of control where a motility of 4 was 100% in the experiment and 0% was a 0 motility score. Bars equal to one Standard Error (SE) n = 6 adult worms per condition. \* = p<0.0001

A)



B)

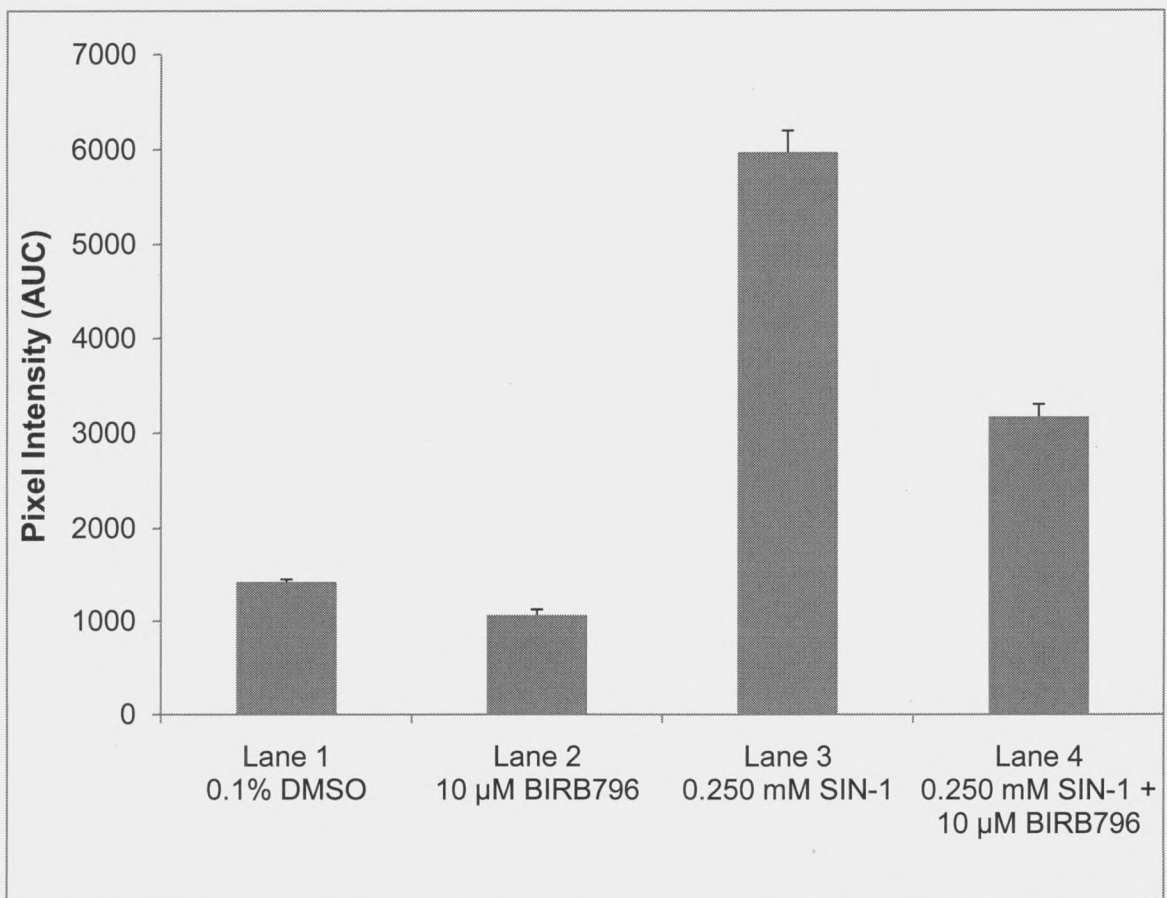


**Figure 8. *In vivo* activation and inhibition of Bm-MPK1.** (A) Western blot was developed using anti-phospho-p38 Rabbit pAb. Each lane was loaded with 26 µg of protein. The treatment group of SIN-1 + BIRB796 was pretreated with BIRB796 for 1 h. (B) The representative pixel intensity of the scanned western blot using Image-J. The pixel intensity was averaged from three separate measurements. Bars equal to one (SE).

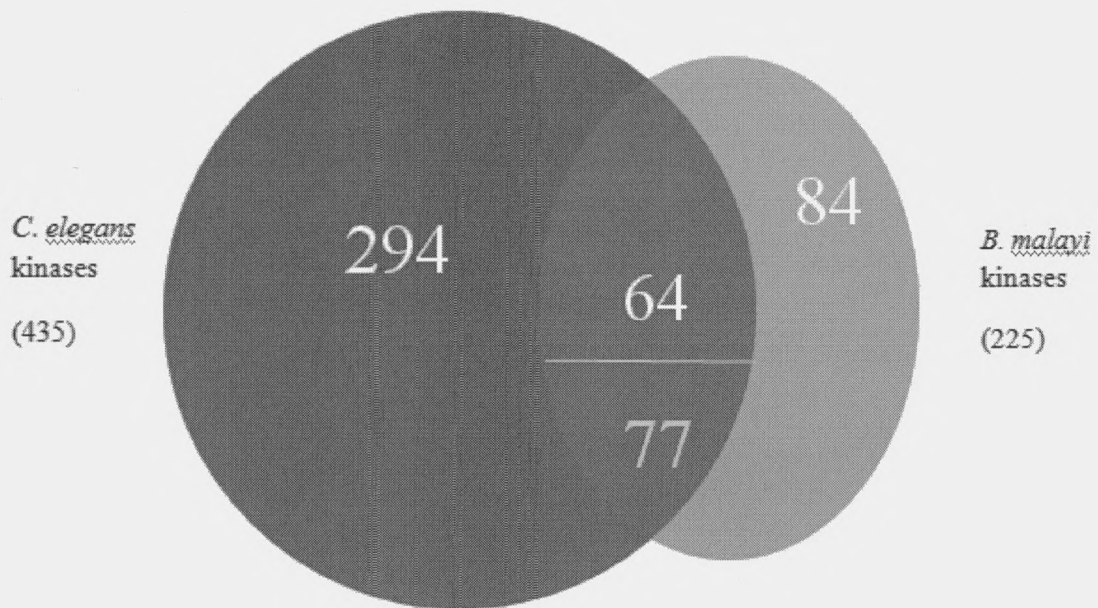


**Figure 9. The kinomes of *C. elegans* and *B. malayi* share 141 kinases.** A total of 435 kinases are present in *C. elegans* and 225 in *B. malayi*. Seventy seven of the 141 shared kinases exhibit detrimental phenotypes.

A)



B)



**Figure 10. Conformational differences in 10  $\mu$ M dasatinib treatment group.** A) The typical elongated conformation of the *B. malayi* parasite. (Scientific Frontline) B) The worm shows a "corkscrew" like conformation as oppose to being elongated. Magnification is at 40x.

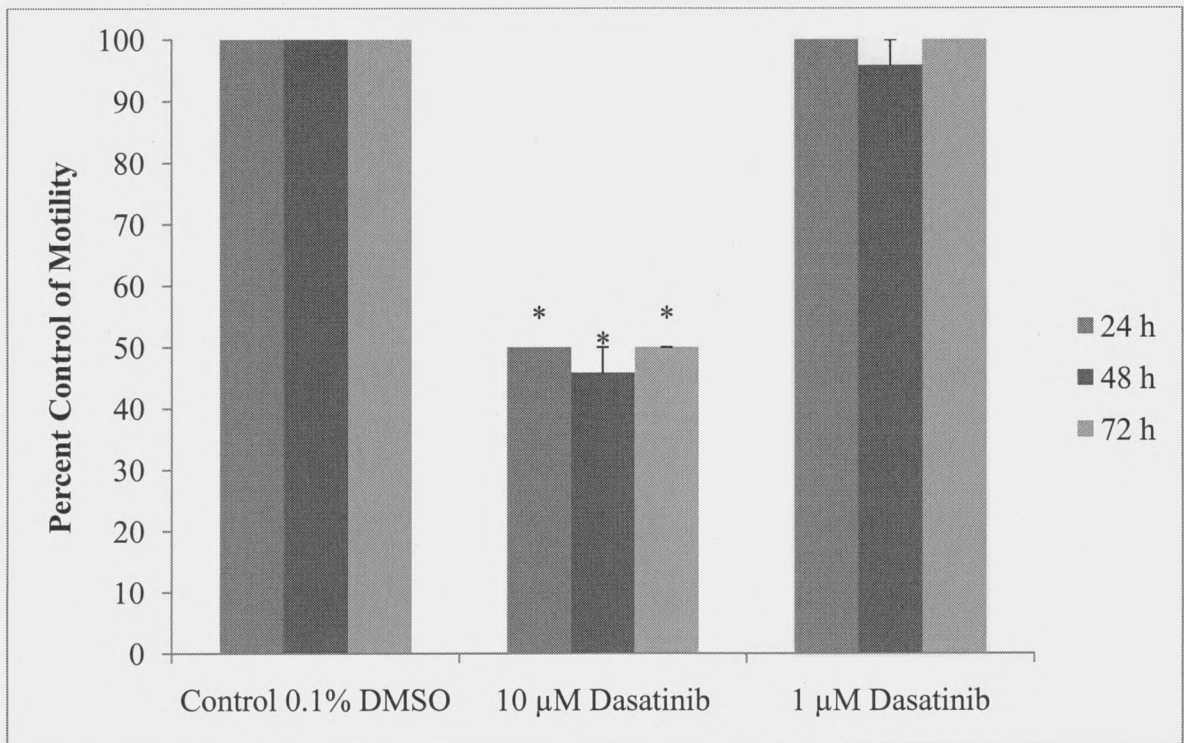


**Figure 11. Effects of dasatinib on adult female *B. malayi* motility.** The data was evaluated as % of control where a motility of 4 was 100% in the experiment and 0% was a 0 motility score. Bars equal to one Standard Error (SE) n = 5 to 6 adult worms per condition. \* = p<0.0001

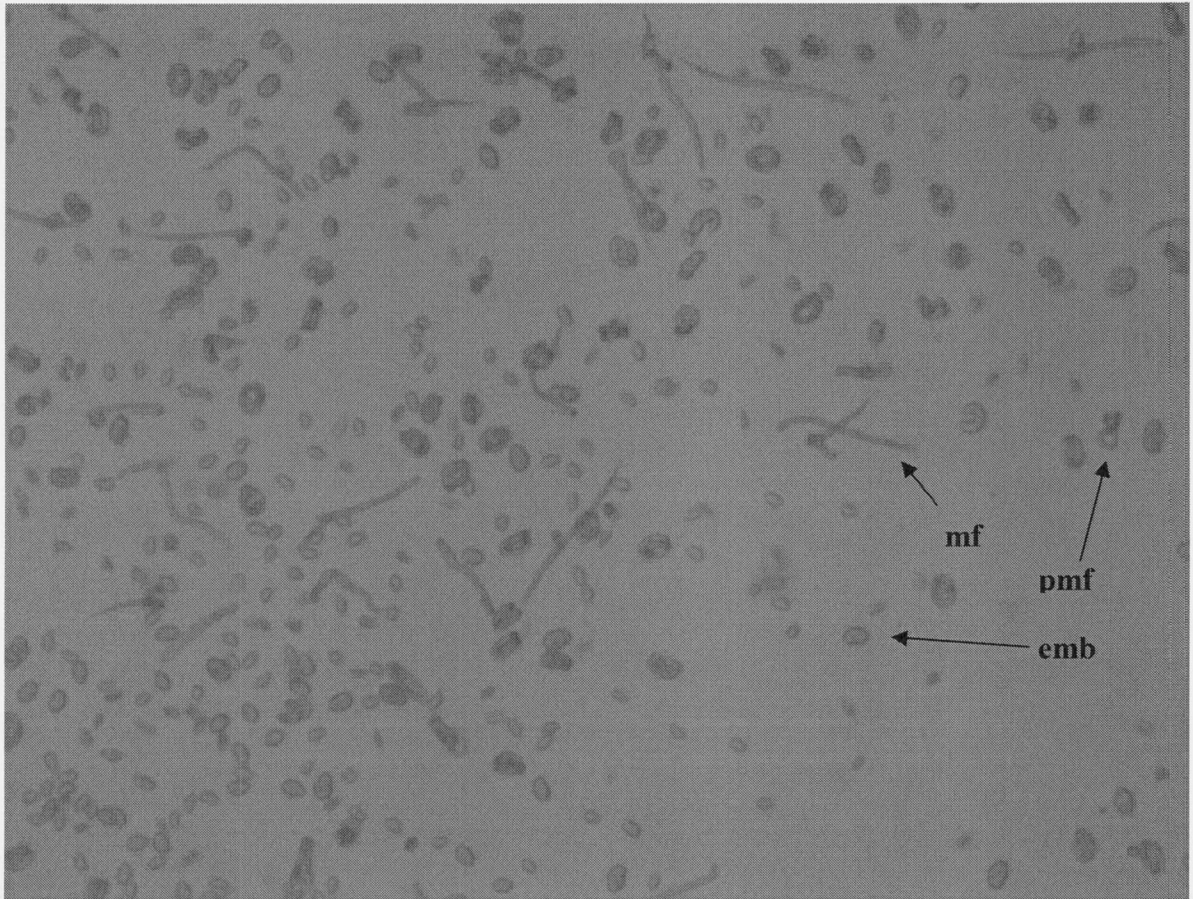


**Figure 12.** The dispersion of microfilaria (mf), premicrofilaria (pmf) and early stage embryos (emb) in the control 0.1% DMSO group. Picture was taken at 50x magnification.

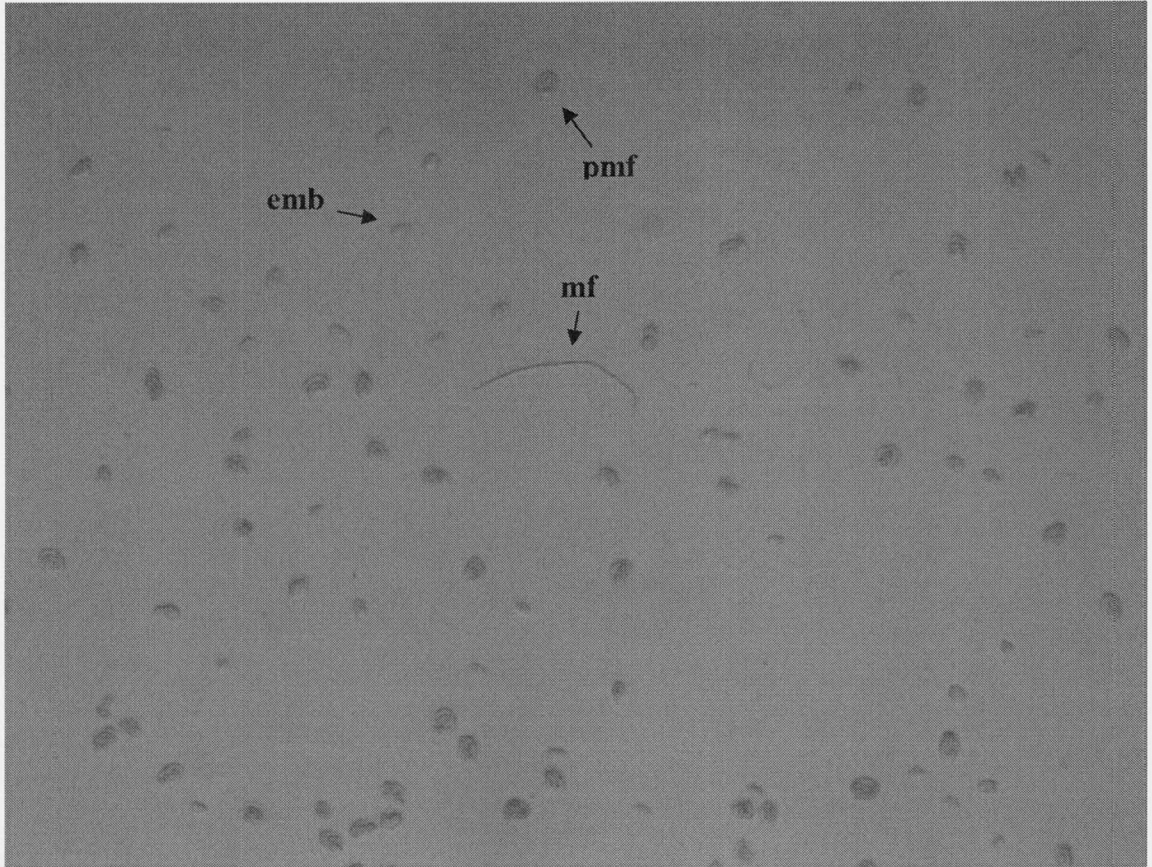


**Figure 13.** The dispersion of microfilaria (mf), premicrofilaria (pmf) and early stage embryos (emb) in the 10  $\mu$ M dasatinib treatment group. Picture was taken at 50x magnification.

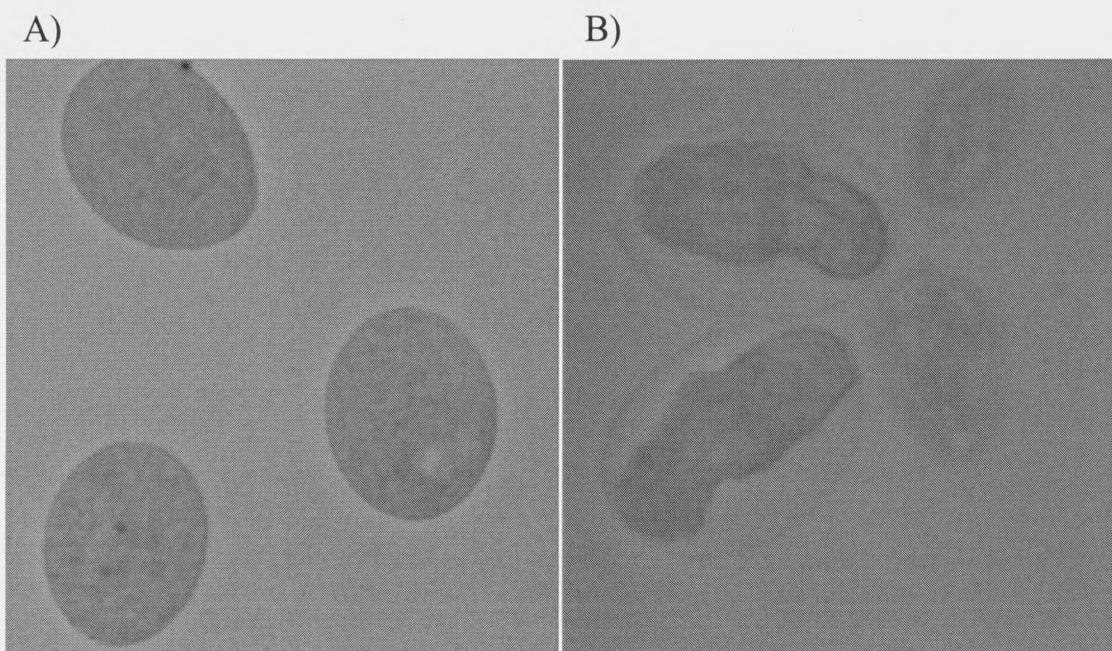


**Figure 14. The phenotypic effects of 10  $\mu$ M dasatinib on early stage embryos in *B. malayi*. A) Control 0.1% DMSO treatment group B) 10  $\mu$ M dasatinib treatment group. Picture was taken at 200x magnification.**

## TABLES

Compound Name	IC <sub>50</sub> (nM)		Ratio (Bm-MPK1/Human p38)
	Human p38	Bm-MPK1	
BIRB796	30	152	5
SB202190	17	220	13
SB203580	15	249	17
VX702	3	4,270	1,420
RWJ67657	4	123	28

**Table 1. IC<sub>50</sub> values of p38 inhibitors against p38 and Bm-MPK1.** The values for human p38 were evaluated previously in the lab.

Samples:	Concentration µg/µl
Control 0.1% DMSO	4.20
10 µM BIRB796	5.08
0.250 mM SIN-1	6.88
0.250 mM SIN-1 + 10 µM BIRB796	5.73

**Table 2. Crude extracts recovered from adult *B. malayi* parasites.** Protein concentrations were measured by Bradford Assay. BSA was used as the standard.



Putative <i>C. elegans</i> ortholog (CDS)	<i>B. malayi</i> (refseq)	RNAi phenotypes (WS219)	Human Ortholog
B0025.1	XP_001893445.1	coelomocyte uptake defective, larval arrest, locomotion variant, slow growth, transgene subcellular localization variant, protein aggregation variant	Phosphoinositide-3-kinase, class 3
B0205.7	XP_001901432.1	male response to contact defective, protruding vulva, embryonic lethal, slow growth, maternal sterile, vulva location variant	CSNK2A1 protein (Casein kinase II alpha 2)
B0207.4	XP_001892118.1	meiotic spindle defective early emb, polar body number defective early emb, locomotion variant, spindle position orientation defective early emb, protein subcellular localization variant, mitotic spindle defective early emb, one cell arrest early emb, chr	Serine/threonine-protein kinase 6
B0218.3	XP_001897803.1	level of transgene expression variant, pathogen susceptibility increased, organism pathogen response variant, cadmium response variant, organism osmotic stress response variant, pathogen induced death increased, pathogen induced cell death reduced	Isoform CSBP2 of Mitogen-activated protein kinase 14
B0240.3	XP_001898315.1	embryonic lethal, slow growth	Atrial natriuretic peptide receptor 1
B0261.2	XP_001901087.1	lipid metabolism variant, growth variant, life span variant, extended life span, gonad development variant, dauer formation variant, translation variant, maternal sterile, hypodermal cell physiology variant, organism heat response variant, slow growth, protein expression reduced, intestinal cell morphology variant, intestinal morphology variant, early larval arrest, embryonic arrest, larval arrest, L3 arrest, embryonic lethal, lysosome organization biogenesis variant, shortened life span, reduced brood size	Serine/threonine-protein kinase mTOR
B0285.1	XP_001900704.1	protruding vulva, sterile, locomotion variant, larval lethal, early larval lethal, slow growth, sterile progeny, organism morphology variant, lethal, larval arrest, embryonic lethal, receptor mediated endocytosis	Isoform 2 of Cell division protein kinase 12

Putative <i>C. elegans</i> ortholog (CDS)	<i>B. malayi</i> (refseq)	RNAi phenotypes (WS219)	Human Ortholog
B0334.8	XP_001902593.1	defective, pattern of transgene expression extended life span, transgene expression increased	Phosphatidylinositol-4,5-bisphosphate 3-kinase catalytic subunit alpha isoform
B0414.7	XP_001901903.1	embryonic lethal, somatic transgene silencing variant, transgene expression increased, RNAi resistant	Mitogen-activated protein kinase kinase 4, isoform CRA b
B0464.5	XP_0019000384.1	sterile, early embryonic lethal, protruding vulva, larval lethal, gametogenesis variant, germline proliferation variant, gonad morphology variant, male mating efficiency reduced, embryonic lethal, sterile F1, cytokinesis variant emb, maternal sterile, few	cDNA FLJ58405, highly similar to Serine/threonine-protein kinase SRPK1
C01G6.8	XP_0019000033.1	protruding vulva, locomotion variant, patchy coloration, vulval cell induction increased, protein expression variant, aldicarb resistant	Tyrosine-protein kinase transmembrane receptor ROR2
C03C10.1	XP_0019000479.1	excess pharyngeal cells, cytoplasmic structure defective early emb, slow growth, E lineage variant, integrity of membranous organelles defective early emb, no gut granules, mitotic spindle defective early emb, embryonic lethal, maternal sterile, transgene	casein kinase 1, alpha 1
C07A9.3	XP_0019000648.1	sterile, embryonic lethal, sick, early larval lethal, small	TLK2 protein
C09D4.3	XP_001895911.1	locomotion variant	tau tubulin kinase 1, isoform CRA c
C10C6.1	XP_001895118.1	embryonic lethal, sterile progeny	microtubule associated serine/threonine kinase 2
C10H11.9	XP_001901340.1	sterile, organism morphology variant, embryonic rupture, embryonic development variant, mid larval arrest, body elongation defective, late embryonic arrest, cortical dynamics defective early emb, neuron positioning variant, dumpy, maternal sterile, cleava	Rho-associated, coiled-coil containing protein kinase 1
C16D9.2	XP_001901842.1	embryonic lethal, locomotion variant, slow growth,	Tyrosine-protein kinase

Putative <i>C. elegans</i> ortholog (CDS)	<i>B. malayi</i> (refseq)	RNAi phenotypes (WS219)	Human Ortholog
C29F9.7	XP_001895617.1	roller paralyzed, locomotion variant, larval lethal, organism morphology variant, body wall muscle myosin organization defective, extended life span, larval arrest, embryonic lethal, paraquat resistant, transgene subcellular localization variant, paralyzed arres	receptor Integrin-linked protein kinase
C32D5.2	XP_001892779.1	slow growth, small, dumpy	bone morphogenetic protein receptor type-1B precursor
C34C6.5	XP_001896987.1	aldicarb resistant	Isoform 1 of Sphingosine kinase 1
C35D10.4	XP_001892048.1	coenzyme Q depleted, mitochondrial metabolism variant, slow growth, sterile progeny, life span variant	Isoform 3 of Chaperone activity of bc1 complex-like, mitochondrial
C41C4.4	XP_001896616.1	level of transgene expression variant, sterile, developmental delay, intestinal vacuole, pharyngeal morphology variant, sick, L2 arrest, tunicamycin response variant, intestinal development variant, unfolded protein response variant, transgene expression extended life span	Isoform 1 of Serine/threonine-protein kinase/endoribonuclease IRE1
C44C8.6	XP_001899387.1	extended life span	MAP kinase-activated protein kinase 3
C46C2.1	XP_001896032.1	egg laying variant, slow growth	WNK lysine deficient protein kinase 1, isoform CRA_b
C48B6.6	XP_001901084.1	excess intestinal cells, protruding vulva, cell proliferation increased	phosphatidylinositol 3-kinase-related protein kinase
D2045.7	XP_001893816.1	maternal sterile	Serine/threonine-protein kinase 16
EEED8.9	XP_001896214.1	transgene subcellular localization variant, protein aggregation variant	Isoform 1 of Serine/threonine-protein kinase PINK1,

Putative <i>C. elegans</i> ortholog (CDS)	<i>B. malayi</i> (refseq)	RNAi phenotypes (WS219)	Human Ortholog
F09E5.1	XP_001892161.1	protruding vulva, asymmetric cell division defective early emb, multivulva, organism morphology variant, cytoskeleton organization biogenesis variant, embryonic lethal, transgene subcellular localization variant, receptor mediated endocytosis defective, maldicarb resistant	mitochondrial Protein kinase C iota type
F15A2.6	XP_001899818.1	late larval lethal, protruding vulva, paralyzed, locomotion variant, slow growth, exploded through vulva	Isoform 4 of BR serine/threonine-protein kinase 2
F19H6.1	XP_001897821.1	age associated fluorescence increased, shortened life span, aldicarb resistant	Serine/threonine-protein kinase Nek7
F20B6.8	XP_001895702.1	protruding vulva, sterile, locomotion variant, slow growth, sterile progeny, lethal, larval arrest, embryonic lethal, maternal sterile, reduced brood size, exploded through vulva	Isoform 1 of Homeodomain-interacting protein kinase 1
F22D6.5	XP_001893916.1	protein subcellular localization variant, chromosome segregation variant, excessive blebbing early emb, age associated fluorescence increased, protruding vulva, P0 spindle absent early emb, slow growth, protein phosphorylation reduced, maternal pronucleus larval lethal	Serine/threonine-protein kinase PRP4 homolog
F28B12.3	XP_001896080.1		Serine/threonine-protein kinase VRK1
F33E2.2	XP_001901143.1	pattern of transgene expression variant, lethal, fat content increased	Isoform 1 of Mitogen-activated protein kinase kinase 13
F39B1.1	XP_001892604.1	apoptosis variant, body wall muscle myosin	Phosphatidylinositol-4-phosphate 3-kinase C2 domain-containing subunit alpha
F42G8.4	XP_001902358.1		Isoform CSBP2 of

Putative <i>C. elegans</i> ortholog (CDS)	<i>B. malayi</i> (refseq)	RNAi phenotypes (WS219)	Human Ortholog
F43C1.2	XP_0019000759.1	organization defective, apoptosis increased sterile, sterile progeny, aldicarb resistant, maternal sterile, protruding vulva, larval lethal, slow growth, sick, multivulva, germ cell mitosis variant, lethal, germline proliferation variant, larval arrest, oocyte septum formation variant, embryonic lethal, meiotic progression during oogenesis variant, shortened life span, reduced brood size	Mitogen-activated protein kinase 14 Mitogen-activated protein kinase 1 (ERK2)
F45H7.4	XP_001899765.1	fat content reduced	Serine/threonine-protein kinase pim-3
F46C3.1	XP_001898944.1	developmental delay, intestinal vacuole, pharyngeal morphology variant, sick, sluggish, L2 arrest, intestinal development variant	Eukaryotic translation initiation factor 2-alpha kinase 3
F46F2.2	XP_001898882.1	seam cell fusion variant, sterile, locomotion variant, alae variant, larval lethal, slow growth, small, organism morphology variant, precocious heterochronic variations, lethal, nicotine hypersensitive, alae secretion variant, embryonic lethal, reduced br	Isoform 1 of Casein kinase I isoform delta
F49B2.5	XP_001899804.1	protruding vulva, larval arrest, sterile, embryonic lethal, sick, oocyte morphology variant, reduced brood size, lethal	Tyrosine-protein kinase FRK Fyn-related kinase (FRK, formerly tyrosine protein kinase 5)
F49E11.1	XP_001899122.1	sterile progeny, protein subcellular localization variant, pronuclear breakdown asynchronous early emb, mitotic spindle defective early emb, multiple nuclei early emb, pseudocleavage exaggerated early emb, excessive blebbing early emb, cell cell contacts	Isoform 1 of Dual specificity tyrosine-phosphorylation-regulated kinase 2
F52C12.2	XP_001898717.1	fat content increased	UPF0293 protein C16orf42
F53G12.6	XP_001897438.1	anoxia hypersensitive	Tyrosine-protein kinase Fer
F55A12.3	XP_001898665.1	defecation cycle variant, larval arrest, no defecation cycle, locomotion variant, sick, maternal sterile	Phosphatidylinositol 4-phosphate 5-kinase type I

Putative <i>C. elegans</i> ortholog (CDS)	<i>B. malayi</i> (refseq)	RNAi phenotypes (WS219)	Human Ortholog
F57F5.5	XP_001901907.1	aldicarb resistant	gamma splice variant 700
F58A3.2	XP_001899548.1	cell secretion variant, sterile, protruding vulva, locomotion variant, slow growth, aldicarb resistant, egg laying variant, embryonic lethal, transgene subcellular localization variant, receptor mediated endocytosis defective, protein expression variant,	Protein kinase C eta type
F59A6.1	XP_001894829.1	level of transgene expression variant, pathogen susceptibility increased, organism pathogen response variant, cadmium response variant, transgene expression reduced	Isoform 20 of Fibroblast growth factor receptor 2
F59E12.2	XP_001893794.1	locomotion variant, embryonic lethal, sterile progeny, protein subcellular localization variant, spindle assembly defective early emb	mitogen-activated protein kinase kinase kinase 15
H37N21.1	XP_001901368.1	egg laying variant, fat content reduced, slow growth	Isoform 1 of Calcium/calmodulin-dependent protein kinase type 1D
H39E23.1	XP_001897380.1	vulva morphology variant, sterile, protruding vulva, asymmetric cell division defective early emb, multivulva, spindle position orientation defective early emb, sterile progeny, ectopic expression transgene, embryonic lethal	Nuclear receptor-binding protein
K03E5.3	XP_001897736.1	locomotion variant, roller, molt defect, small, organism morphology variant, germ cell mitosis variant, larval arrest, embryonic lethal, exploded through vulva	Isoform 1 of Serine/threonine-protein kinase MARK2
K08B12.5	XP_001891968.1	locomotion variant, slow growth, dumpy, organism morphology variant	serine/threonine kinase (CDC2/CDKX subfamily)
M01B12.5	XP_001901329.1	protruding vulva, sterile, larval lethal, slow growth, sick, small, lethal, fat content reduced, larval arrest, embryonic lethal, receptor mediated endocytosis defective, reduced brood size, pattern of transgene	Isoform 3 of Serine/threonine-protein kinase MRCK alpha
			Serine/threonine-protein kinase RIO1

Putative <i>C. elegans</i> ortholog (CDS)	<i>B. malayi</i> (refseq)	RNAi phenotypes (WS219)	Human Ortholog
M79.1	XP_001897557.1	expression variant apoptosis reduced, organism ionizing radiation response variant, pathogen resistance increased, germ cell hypersensitive ionizing radiation	Isoform IB of Tyrosine-protein kinase ABL1
R03G5.2	XP_001899453.1	level of transgene expression variant, organism pathogen response variant, cadmium response variant	Isoform 1 of Dual specificity mitogen-activated protein kinase kinase 6
T01C8.1	XP_001901488.1	extended life span, age associated fluorescence increased, shortened life span, dauer constitutive	5'-AMP-activated protein kinase catalytic subunit alpha-2
T04B2.2	XP_001900551.1	embryonic lethal, embryonic development variant, fat content increased	Tyrosine-protein kinase Fer
T04C10.1	XP_001898840.1	locomotion variant, slow growth	Isoform 1 of Dual specificity tyrosine-phosphorylation-regulated kinase 1A
T05G5.3	XP_001891803.1	sterile, one cell shape defective early emb, locomotion variant, endoplasmic reticulum morphology variant, sterile progeny, cell cycle slow early emb, one cell arrest early emb, pronuclear migration defective early emb, maternal sterile, oogenesis variant	cell division control protein 2 homolog isoform 1
T07F12.4	XP_001902378.1	transgene subcellular localization variant, protein aggregation variant	serine/threonine-protein kinase ULK2
T10H9.2	XP_001901874.1	slow growth	ALK tyrosine kinase receptor precursor
T17E9.1	XP_001902941.1	locomotion variant, larval lethal, slow growth, organism morphology variant, aldicarb resistant, embryonic lethal, dumpy, maternal sterile, reduced brood size	Isoform 1 of Serine/threonine-protein kinase TAO1
W03A5.1	XP_001898197.1	embryonic lethal, slow growth	Tyrosine-protein kinase FRK Fyn-related kinase

Putative <i>C. elegans</i> ortholog (CDS)	<i>B. malayi</i> (refseq)	RNAi phenotypes (WS219)	Human Ortholog
W04B5.5	XP_001897080.1	sterile, larval arrest, embryonic lethal, reduced brood size, thin	(FRK, formerly tyrosine protein kinase 5) 3-phosphoinositide-dependent protein kinase 1 isoform 1
W06B3.2	XP_001892881.1	growth variant, gut granule development variant, small	Isoform 1 of Mitogen-activated protein kinase 7
W06F12.3	XP_001897369.1	slow growth	Isoform 3 of Tau-tubulin kinase 2
W09C5.5	XP_001896679.1	locomotion variant, amplitude of movement variant	Serine/threonine-protein kinase D2
Y92H12A.1	XP_001898655.1	<b>locomotion variant</b> , protein phosphorylation reduced, intestinal development variant, lethal, mitotic spindle <b>defective early emb</b> , gonad development variant, embryonic lethal, protein expression variant, distal tip cell migration variant	Isoform 1 of Tyrosine-protein kinase Fyn (scr-1)
Y106G6E.6	XP_001898636.1	spindle orientation defective early emb, sterile, paralyzed, protruding vulva, locomotion variant, larval lethal, slow growth, small, organism morphology variant, aldicarb resistant, egg laying variant, embryonic lethal, reduced brood size, dumpy	Isoform 1 of Casein kinase I isoform gamma-3
Y52D3.1	XP_001900783.1	embryonic lethal, ventral cord patterning variant, axon midline crossing variant, cord commissures fail to reach target	STE20-related kinase adapter protein alpha isoform 4
ZC504.4	XP_001897953.1	protruding vulva, locomotion variant, fat content reduced, cell migration variant, pattern of transgene expression variant, receptor mediated endocytosis defective, developmental delay postembryonic, distal tip cell migration variant	Isoform 3 of Mitogen-activated protein kinase kinase kinase 4
ZC581.1	XP_001902607.1	sterile, locomotion variant, slow growth, larval lethal, roller, organism morphology variant, protein aggregation variant, larval arrest, late larval lethal,	Serine/threonine-protein kinase Nek8



Putative <i>C. elegans</i> ortholog (CDS)	<i>B. malayi</i> (refseq)	RNAi phenotypes (WS219)	Human Ortholog
ZC581.9	XP_001892158.1	transgene subcellular localization variant ventral cord patterning variant, axon midline crossing variant, axon fasciculation variant, cord commissures fail to reach target	SCY1-like protein 2
ZK1067.1	XP_001901212.1	gonad sheath contraction rate reduced, ovulation variant, quiescence variant	Isoform 1 of Epidermal growth factor receptor
ZK370.5	XP_001897480.1	aldicarb resistant	[Pyruvate dehydrogenase [lipoamide]] kinase isozyme 2, mitochondrial
ZK930.1	XP_001896013.1	fat content reduced	Phosphoinositide 3-kinase regulatory subunit 4

**Table 3. Seventy-seven kinases that are orthologous in *C. elegans*, *B. malayi* and Humans.** The phenotype of the RNAi knockdown in *C. elegans* is described. The *scr-1* gene is highlighted

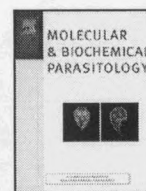
## REFERENCES

1. Singh, P.K., et al., *Towards novel antifilarial drugs: challenges and recent developments*. Future Medicinal Chemistry, 2010. **2**(2): p. 251-283.
2. Bockarie, M.J., M.J. Taylor, and J.O. Gyapong, *Current practices in the management of lymphatic filariasis*. Expert Rev Anti Infect Ther, 2009. **7**(5): p. 595-605.
3. Paily, K., S. Hoti, and P. Das, *A review of the complexity of biology of lymphatic filarial parasites*. Journal of Parasitic Diseases, 2009. **33**(1): p. 3-12.
4. Tompkins, J.B., L.E. Stitt, and B.F. Ardelli, *Brugia malayi: in vitro effects of ivermectin and moxidectin on adults and microfilariae*. Exp Parasitol, 2010. **124**(4): p. 394-402.
5. McGarry, H.F., L.D. Plant, and M.J. Taylor, *Diethylcarbamazine activity against Brugia malayi microfilariae is dependent on inducible nitric-oxide synthase and the cyclooxygenase pathway*. Filaria J, 2005. **4**: p. 4.
6. Rao, U.R., et al., *Brugia malayi and Acanthocheilonema viteae: antifilarial activity of transglutaminase inhibitors in vitro*. Antimicrob. Agents Chemother., 1991. **35**(11): p. 2219-2224.
7. Lustigman, S. and J.P. McCarter, *Ivermectin resistance in Onchocerca volvulus: toward a genetic basis*. PLoS Negl Trop Dis, 2007. **1**(1): p. e76.
8. Geary, T.G., et al., *Unresolved issues in anthelmintic pharmacology for helminthiasis of humans*. Int J Parasitol, 2010. **40**(1): p. 1-13.
9. Patel, A., et al., *The role of a Brugia malayi p38 MAP kinase ortholog (Bm-MPK1) in parasite anti-oxidative stress responses*. Molecular and Biochemical Parasitology, 2011. **176**(2): p. 90-97.

10. Maizels, R.M., M.L. Blaxter, and A.L. Scott, *Immunological genomics of Brugia malayi: filarial genes implicated in immune evasion and protective immunity*. Parasite Immunol, 2001. **23**(7): p. 327-44.
11. Awasthi, S.K., et al., *Antifilarial activity of 1,3-diarylpropen-1-one: effect on glutathione-S-transferase, a phase II detoxification enzyme*. Am J Trop Med Hyg, 2009. **80**(5): p. 764-8.
12. Mittelstadt, P.R., et al., *Activating p38 MAPK: new tricks for an old kinase*. Cell Cycle, 2005. **4**(9): p. 1189-92.
13. Cuenda, A. and S. Rousseau, *p38 MAP-kinases pathway regulation, function and role in human diseases*. Biochim Biophys Acta, 2007. **1773**(8): p. 1358-75.
14. Lee, J.C., et al., *Inhibition of p38 MAP kinase as a therapeutic strategy*. Immunopharmacology, 2000. **47**(2-3): p. 185-201.
15. Kumar, S., J. Boehm, and J.C. Lee, *p38 MAP kinases: key signalling molecules as therapeutic targets for inflammatory diseases*. Nat Rev Drug Discov, 2003. **2**(9): p. 717-26.
16. Coulthard, L.R., et al., *p38(MAPK): stress responses from molecular mechanisms to therapeutics*. Trends Mol Med, 2009. **15**(8): p. 369-79.
17. Pargellis, C., et al., *Inhibition of p38 MAP kinase by utilizing a novel allosteric binding site*. Nat Struct Biol, 2002. **9**(4): p. 268-72.
18. Inoue, H., et al., *The C. elegans p38 MAPK pathway regulates nuclear localization of the transcription factor SKN-1 in oxidative stress response*. Genes Dev, 2005. **19**(19): p. 2278-83.
19. An, J.H., et al., *Regulation of the Caenorhabditis elegans oxidative stress defense protein SKN-1 by glycogen synthase kinase-3*. Proc Natl Acad Sci U S A, 2005. **102**(45): p. 16275-80.
20. Troemel, E.R., et al., *p38 MAPK regulates expression of immune response genes and contributes to longevity in C. elegans*. PLoS Genet, 2006. **2**(11): p. e183.

21. Available from: <http://www.invitrogen.com/site/us/en/home/References/Molecular-Probes-The-Handbook/Probes-for-Reactive-Oxygen-Species-Including-Nitric-Oxide/Probes-for-Nitric-Oxide-Research.html>.
22. Li, C.Q., et al., *Threshold effects of nitric oxide-induced toxicity and cellular responses in wild-type and p53-null human lymphoblastoid cells*. Chem Res Toxicol, 2006. **19**(3): p. 399-406.
23. Selkirk, M.E., et al., *Resistance of filarial nematode parasites to oxidative stress*. Int J Parasitol, 1998. **28**(9): p. 1315-32.
24. Szabo, C., H. Ischiropoulos, and R. Radi, *Peroxynitrite: biochemistry, pathophysiology and development of therapeutics*. Nat Rev Drug Discov, 2007. **6**(8): p. 662-680.
25. Liotta, F. and J.J. Siekierka, *Apicomplexa, trypanosoma and parasitic nematode protein kinases as antiparasitic therapeutic targets*. Curr Opin Investig Drugs, 2010. **11**(2): p. 147-56.
26. Manning, G., *Genomic overview of protein kinases*. WormBook, 2005: p. 1-19.
27. Ghedin, E., et al., *Draft genome of the filarial nematode parasite Brugia malayi*. Science, 2007. **317**(5845): p. 1756-60.
28. Geldhof, P., et al., *RNA interference in parasitic helminths: current situation, potential pitfalls and future prospects*. Parasitology, 2007. **134**(Pt 5): p. 609-19.
29. Knox, D.P., et al., *RNA interference in parasitic nematodes of animals: a reality check?* Trends Parasitol, 2007. **23**(3): p. 105-7.
30. Jezequel-Sur, S., et al., *Mixing two differently labeled substrates in one immobilized metal assay for phosphochemicals assay to improve data quality*. Analytical Biochemistry, 2007. **360**(2): p. 312-314.

31. Bradford, M.M., *A rapid and sensitive method for the quantitation of microgram quantities of protein utilizing the principle of protein-dye binding*. Anal Biochem, 1976. **72**: p. 248-54.
32. Collins, T.J., *ImageJ for microscopy*. Biotechniques, 2007. **43**(1 Suppl): p. 25-30.
33. Comley, J.C., et al., *Colorimetric quantitation of filarial viability*. Int J Parasitol, 1989. **19**(1): p. 77-83.
34. Brunet, L.R., *Nitric oxide in parasitic infections*. Int Immunopharmacol, 2001. **1**(8): p. 1457-67.
35. Guner, Y.S., et al., *Peroxynitrite-induced p38 MAPK pro-apoptotic signaling in enterocytes*. Biochem Biophys Res Commun, 2009. **384**(2): p. 221-5.
36. Jope, R.S., L. Zhang, and L. Song, *Peroxynitrite modulates the activation of p38 and extracellular regulated kinases in PC12 cells*. Arch Biochem Biophys, 2000. **376**(2): p. 365-70.



## The role of a *Brugia malayi* p38 MAP kinase ortholog (Bm-MPK1) in parasite anti-oxidative stress responses

Akruti Patel, Agnieszka Nawrocka Chojnowski, Katie Gaskill, William De Martini, Ronald L. Goldberg, John J. Siekierka\*

Department of Chemistry and Biochemistry and The Herman and Margaret Sokol Institute for Pharmaceutical Life Sciences, Montclair State University, Montclair, NJ 07043, USA

### ARTICLE INFO

#### Article history:

Received 11 November 2010  
Received in revised form  
15 December 2010  
Accepted 20 December 2010  
Available online 24 December 2010

#### Key words:

Filarial parasites  
*Brugia malayi*  
Stress-activated protein kinases  
P38 MAPK orthologs  
Reactive oxygen species

### ABSTRACT

Filariasis, caused by thread-like nematode worms, affects millions of individuals throughout the tropics and is a major cause of acute and chronic morbidity. Filarial nematodes effectively evade host immunological responses and are long lived within their hosts. Recently an emphasis has been placed on enzymatic and non-enzymatic anti-oxidant systems which counteract the generation of reactive oxygen species (ROS) by macrophages and granulocytes, a first line of defense against parasites. We have characterized an anti-oxidant pathway in the filarial parasite *Brugia malayi* related to the evolutionarily conserved human mitogen-activated p38 protein kinase and the *Caenorhabditis elegans* PMK-1 protein kinase stress pathways. We have expressed a recombinant p38/PMK-1 ortholog from *B. malayi* (Bm-MPK1) and have successfully activated the kinase with mammalian upstream kinases. In addition, we have demonstrated inhibition of Bm-MPK1 activity using a panel of known p38 inhibitors. Using the potent and highly selective allosteric p38 inhibitor, BIRB796, we have implicated Bm-MPK1 in a pathway which offers *B. malayi* protection from the effects of ROS. Our results, for the first time, describe a stress-activated protein kinase pathway within the filarial parasite *B. malayi* which plays a role in protecting the parasite from ROS. Inhibition of this pathway may have therapeutic benefit in treating filariasis by increasing the sensitivity of filarial parasites to ROS and other reactive intermediates.

Published by Elsevier B.V.

### 1. Introduction

Pathogenic filarial nematodes affect the lives of over 120 million people and place over one billion people at risk of infection [1,2]. Filarial diseases have a significant economic and psychosocial impact in endemic areas, disfiguring and incapacitating millions of individuals. The filarial parasites that pose the most serious public health threats are *Wuchereria bancrofti*, *Brugia malayi* and *Brugia timori*, the causative agents of lymphatic filariasis (elephantiasis), as well as *Onchocerca volvulus* and *Loa loa*, the causative agents of subcutaneous filariasis (e.g. river blindness). In spite of some success in treating filarial diseases with Mectizan® (ivermectin), albendazole, and diethylcarbamazine, there is a need for new drugs. Current drugs target the immature stages (microfilariae) but not the long-lived adult worms. There is also significant toxicity associated with using these drugs and drug resistance is emerging [3,4]. Identification of new therapeutic agents for the treatment of filarial disease requires a better understanding of filarial homeostasis and critical

parasite biochemical pathways amiable to drug targeting, an effort greatly enhanced with the sequencing of the *B. malayi* genome [5].

Our laboratory has been studying protective responses to oxidative stress in the filarial parasite *B. malayi*. Filarial and other parasites exhibit a number of defense mechanisms permitting the parasite to establish infection in the presence of host immune responses, allowing for long term survival within the host [6–9]. One response used by the host to thwart infection is the generation of reactive oxygen species (ROS) by macrophages, neutrophils, eosinophils and basophil granulocytes which can cause severe damage to the parasites through oxidation of proteins, lipids, and nucleic acids. Filarial parasites have elaborated a number of antioxidant mechanisms and are known to effectively evade oxidative stress mediated by ROS [9,10]. It has been demonstrated that for the distantly related non-parasitic nematode, *Caenorhabditis elegans*, the critical pathway for dealing with oxidative stress, detoxification of xenobiotics as well as innate immunity, involves a protein kinase called PMK-1 [12–14]. PMK-1 is a *C. elegans* ortholog of the human stress-activated protein kinase p38 (p38), and a member of the mitogen-activated protein kinase (MAPK) superfamily. Human p38 is a serine/threonine protein kinase, consisting of four isoforms (p38 $\alpha$ ,  $\beta$ ,  $\gamma$  and  $\delta$ ) that play important roles in cellular responses

\* Corresponding author. Tel.: +1 973 655 3411; fax: +1 973 655 7772.  
E-mail address: siekierkaj@mail.montclair.edu (J.J. Siekierka).

	I	II	
<i>B. malayi</i>	-----MELTRTLKPGFYAVELNKTWIIIPNICYQLNTPVGTGAYGTVCAAECPRTGKVAIKKFSRPFQSAIH	67	
<i>W. bancrofti</i>	-----MELTRTLKPGFYAVELNKTWIIIPNICYQLNTPVGTGAYGTVCAAECPRTGKVAIKKFSRPFQSAIH	67	
<i>L. loa</i>	-----MELTRTLKLGFYAVELNKTWIIIPNYYQLNTPVGTGAYGTVCAAECPRTGKVAIKKFSRPFQSAIH	67	
<i>C. elegans</i>	MFPQTTMDHILHPTPREGYYVVELNRSVWVVPNYIINLTPIGTGAYGTVCAAECPRTGKVAIKKFSRPFQSAIH	75	
<i>H. sapiens</i>	-----MSQERPTFYRQLNKTIIWEVPERYQNLSPVGSYGYSVCAAFDTKTGLRVAVKLSRPFQSAIH	64	
<i>E. multicularis</i>	-----MPDVNERRFVFEINQLRWDLPDRYTPVNVAGQGSFGTVSSAFDKYLQREVAIKKLDLRRPFENAEF	65	
	III	IV	V
<i>B. malayi</i>	AKRTHRELKLLRSMNHENIIDMLDVFTPDINATSLQDVYFVSMMLGADLSSILKIQRLSDDDHIQFLVYQILRGLK	142	
<i>W. bancrofti</i>	AKRTHRELKLLRSMNHENIIDMLDVFTPDINATSLQDVYFVSMMLGADLSSILKIQRLSDDDHIQFLVYQILRGLK	142	
<i>L. loa</i>	AKRTHRELKLLRSMNHENIIDMLDVFTPDINATSLQDVYFVSMMLGADLSSILKIQRLSDDDHIQFLVYQILRGLK	142	
<i>C. elegans</i>	ARRTYRELRLLRSMCHENIIDMLDVFTPNENVNDIEDVYFVSMMLGADLSSILKIQRLSDDDHIQFLVYQILRGLK	150	
<i>H. sapiens</i>	AKRTYRELRLKHKMKHENVIGLLDVFTPARSLEEFNDVYLVTHLMGADLNNIKKQKQLTDDHVOFLIYQILRGLK	139	
<i>E. multicularis</i>	AKRTYRELRLAQMHDHENVICLIDAFPTQTSLETTFEDVYLVTPMLDADLGAIVAQQVLTDDQICFLAYQMLRALK	140	
	VIa		
<i>B. malayi</i>	YIHSAGLIHRDLKPSNIAVNEDECLEKI LDFGLARQTDSEM <b>TGY</b> VATRWYRAPEIMLNWMHYTQTVDIWSVGCIMA	217	
<i>W. bancrofti</i>	YIHSAGLIHRDLKPSNIAVNEDECLEKI LDFGLARQTDSEM <b>TGY</b> VATRWYRAPEIMLNWMHYTQTVDIWSVGCIMA	217	
<i>L. loa</i>	YIHSAGLIHRDLKPSNIAVNEDECLEKI LDFGLARQTDSEM <b>TGY</b> VATRWYRAPEIMLNWMHYTQTVDIWSVGCIMA	217	
<i>C. elegans</i>	YIHSADIIHRDLKPSNIAVNEDECLEKI LDFGLARQTDSEM <b>TGY</b> VATRWYRAPEIMLNWMHYTQTVDVWSVGCILA	225	
<i>H. sapiens</i>	YIHSADIIHRDLKPSNIAVNEDECLEKI LDFGLARHTDDEM <b>TGY</b> VATRWYRAPEIMLNWMHYNTQTVDIWSVGCIMA	214	
<i>E. multicularis</i>	YMHGAHIIHRDLKPSNIGVNSDVELRIIDFGLARQKNHLM <b>TGY</b> VATRWYRAPEVMLNWMHYNSVDVWSVACILV	215	
	VIb	VII	VIII
<i>B. malayi</i>	ELITGRTLFPFGADHIDQLTRIMNVVGTPEEFLSKIQSDEARNYIRNLPKTPRKDFKRLFPASFPDAIDLLERTL	292	
<i>W. bancrofti</i>	ELITGRTLFPFGADHIDQLTRIMNVVGTPEEFLSKIQSDEARNYIRNLPKTPRKDFKRLFPASFPDAIDLLERTL	292	
<i>L. loa</i>	ELITGRTLFPFGADHIDQLTRIMNVVGTPEEFLSKIQSDEARNYIRNLPKTPRKDFKRLFPASFPDAIDLLERTL	292	
<i>C. elegans</i>	ELITGKTLFPFGSDHIDQLTRIMSVTGTPEEFLKKSISEEARNYIRNLPKTPRRDFKRLFAQATPQADLLEKML	300	
<i>H. sapiens</i>	ELITGRTLFPFGTDHIDQLKILRLVGTPGAELLKKSISEEARNYIQSLTQMPKMFANVFIGANPLAVDLLEKML	289	
<i>E. multicularis</i>	ELKTRQPLFRGLNHDQVKQIMSIVGAPDEELMOKITSSSAREFIEKLNYSKKDLKDAFFWASEVLLDLSKML	290	
	X		
<i>B. malayi</i>	NLDPDYRPTASEAMEHFYLYKQYHDPSPVSPPLDID-SDG-DLTIQWK	340	
<i>W. bancrofti</i>	NLDPDYRPTASEAMEHFYLYKQYHDPSPVSPPLDID-SDG-DLTIQWK	340	
<i>L. loa</i>	NLDPDYRPTASEAMEHFYLYKQYHDPSPVSPPLDID-SDG-DLTIQWK	340	
<i>C. elegans</i>	HLDPDRPTAKEAMEHEYLAAHYHDETDEPIAEEMDLN-DDVRADTIDEWK	349	
<i>H. sapiens</i>	VLDSDKRI TAAQALAHAYFAQYHDPDPEVADPYDQS-FESRDLLEDEWK	338	
<i>E. multicularis</i>	VLDPDRRLTAAQALAHFYFAEYHNESDEPVGEPLDDLIDSDNLTMEEWK	340	
	XI		

**Fig. 1.** Clustal W alignment of human and nematode p38 MAPK catalytic domains. Highly conserved segments are highlighted in grey. Roman numerals indicate MAPK subdomain regions. The TGY dual phosphorylation motif is highlighted in bold font (arrow). The corresponding accession numbers are: *Brugia malayi*: Bm-MPK1, A8PQ50; *Wuchereria bancrofti* CMGC/MAPK/p38 protein kinase, WUBG\_01668.1/WUBG14523.1 (Broad Institute Filial Database); *Loa loa* CMGC/MAPK/p38 protein kinase, LOAG.06056.1 (Broad Institute Filial Database); *Caenorhabditis elegans* PMK-1, Q17446; Human p38 $\alpha$  (MAPK14), Q16539; *E. multicularis* EmMPK2, B1VK39.

to external stress signals including osmotic stress, viral infection, ultraviolet light, heat, and inflammatory cytokines [15]. Activation of upstream kinases, such as apoptosis signal-regulating kinase 1 (ASK-1), in response to stress leads to the activation of mitogen-activated protein kinase kinases 3 and 6 (MKK3 and MKK6) which dually phosphorylate the TGY motif within the phosphorylation lip of p38, leading to its activation. Activated p38 subsequently phosphorylates and activates several downstream protein kinases and transcription factors involved in the regulation of genes that mediate a variety of anti-stress responses [15]. Similarly, PMK-1 is activated by dual phosphorylation of a TGY motif by SEK-1, an ortholog of MKK6, in turn leading to the phosphorylation of SKN-1, a transcription factor involved in mesodermal specification and oxidative stress responses [12,16]. In this study, we report for the first time the characterization of a closely related p38/PMK-1 ortholog expressed in the filarial parasite, *B. malayi*, which we termed Bm-MPK1. Bm-MPK1 orthologs are present in other filarial parasites such as *W. bancrofti* and *L. loa* as well as other, non-filarial parasites, such as *Echinococcus multilocularis* (Fig. 1). Bm-MPK1 and its orthologs exhibit the characteristic 12 domain structure of the mitogen-activated protein kinase family as well as the highly conserved TGY activation motif in domain VIII (Fig. 1). It should be noted that protozoal parasite protein kinases, including stress-activated protein kinases, have been receiving significant attention as potential therapeutic targets [17].

## 2. Materials and methods

### 2.1. Generation of vectors expressing Bm-MPK1

The full length Bm-MPK1 sequence was obtained from the UniProt protein database (EMBL-EBI accession no. A8PQ50). The human codon-optimized *bm-MPK1* gene was produced synthetically (Blue Heron Biotechnology, Bothell, WA) and cloned into the Gateway<sup>®</sup> system pDONR<sup>TM</sup>221 entry vector (Invitrogen, Carlsbad, CA). The *bm-MPK1* gene was initially cloned into plasmid pDONR<sup>TM</sup>221 and then transferred into a pDEST<sup>TM</sup>27 mammalian expression vector using *in vitro* LR recombination reaction as per the manufacturer's instructions, ultimately producing Bm-MPK1/pDEST<sup>TM</sup>27. The pDEST<sup>TM</sup>27 vector is an N-terminal Glutathione S-transferase (GST) fusion vector that generates an N-terminal GST tagged protein. Plasmid DNA concentration was determined using Hoechst 33258 dye assay [18].

### 2.2. Expression of recombinant Bm-MPK1

FreeStyle<sup>TM</sup> 293-F cells (HEK 293F, Invitrogen) were maintained in 125 mL polycarbonate Erlenmeyer flasks containing Freestyle<sup>TM</sup> 293 expression medium (Invitrogen) in a 37 °C humidified incubator on an orbital shaker platform (135 rpm) with 8% CO<sub>2</sub>. Cells were subcultured once the cell density reached 2–3 × 10<sup>6</sup> viable

cells/mL ensuring >90% cell viability for all experiments. The cell density and the viability of cells were determined by counting the cells using the trypan blue exclusion method [19]. Cells were transfected with the Bm-MPK1/pDEST<sup>TM</sup>27 expression vector using FreeStyle<sup>TM</sup> 293fectin Reagent (Invitrogen) or FreeStyle<sup>TM</sup> MAX Reagent (Invitrogen) according to the manufacturer's directions. Forty-eight hours later, HEK 293F cells were treated with 400  $\mu$ M sodium arsenate ( $\text{Na}_2\text{HAsO}_4$ , MP Biomedicals, Solon, Ohio) for 3 h to activate recombinant Bm-MPK1 [20]. Transfected cells were centrifuged at  $100 \times g$  for 5 min and washed twice in cold phosphate buffered saline (PBS) prior to being lysed in 2.0 mL of cold lysis buffer [10 mM HEPES pH 7.4, 50 mM  $\beta$ -glycerolphosphate, 1% Triton X-100, 10% glycerol, 2 mM EDTA, 2 mM EGTA, 1 mM DTT, 10 mM NaF and 1:100 Halt<sup>TM</sup> Protease Inhibitor Cocktail (Thermo-Fisher Scientific, Rockford, IL)] for every  $50\text{--}100 \times 10^6$  cells. Alternatively, 1.0 mL of commercial M-PER<sup>®</sup> Mammalian Protein Extraction Reagent (Thermo-Fisher Scientific) per 100 mg ( $\sim 100 \mu\text{L}$ ) of cell pellet with 1:100 Halt<sup>TM</sup> Protease Inhibitor Cocktail (Thermo-Fisher Scientific) was used. Cell-free lysates were clarified by centrifugation at  $14,000 \times g$  for 10 min prior to use. Negative control lysates were prepared from cells transfected with pDEST<sup>TM</sup>27.

### 2.3. Purification of GST-tagged Bm-MPK1

GST-tagged Bm-MPK1 was purified at 4 °C using HighAffinity GST Resin (0.5–1.0 mL resin, GenScript, Piscataway, NJ) in a small column. The column was equilibrated with 10 resin bed volumes of PBS. Cell lysates were added to the GST resin which was re-suspended and incubated for 1 h with mixing on a tube rotator to allow protein binding. The column was washed 4 times with 2 mL of PBS and fractions were monitored by absorbance at 280 nm. The column was washed once with 2 mL of buffer A (25 mM HEPES, 150 mM NaCl, 1 mM DTT, 10% glycerol, 0.1 mM EDTA, 1:100 Halt<sup>TM</sup> Protease Inhibitor Cocktail). Protein was eluted with 5 resin bed volumes of buffer A supplemented with 10 mM reduced L-glutathione (Sigma–Aldrich, St. Louis, MO). Fractions were analyzed for protein using the Bradford assay (Sigma–Aldrich), according to the manufacturer's instructions, with bovine serum albumin (BSA) as a standard.

### 2.4. SDS-PAGE and Western blotting of Bm-MPK1 protein

Bm-MPK1 protein samples were analyzed using SDS gel electrophoresis (SDS-PAGE). Samples were prepared in NuPAGE<sup>®</sup> SDS Sample Buffer (Invitrogen) containing NuPAGE<sup>®</sup> Reducing Agent (Invitrogen) and incubated at 90 °C for 5 min prior to loading them on a NuPAGE<sup>®</sup> 4–12% Bis-Tris gel (Invitrogen). Gels were run at constant voltage (200 V) for 40 min in MOPS-SDS running buffer (Invitrogen) using Novex<sup>®</sup> Sharp Pre-Stained Protein Standards (Invitrogen) or MagicMark<sup>TM</sup> XP Western Standard (Invitrogen) molecular weight markers. Gels were stained for 1 h with staining solution (0.05% Coomassie Blue R-250, 5% acetic acid, 44% methanol) and destained with a 50% methanol–10% acetic acid solution for 30 min followed by a 1 h incubation in 5% acetic acid.

Protein was transferred from SDS-PAGE gels on to polyvinylidene difluoride (PVDF) membrane using NuPAGE<sup>®</sup> Transfer Buffer (Invitrogen) containing 10% methanol and 0.25% SDS using a TE77XP Semi-Dry Blotter (Hoefer, Holliston, MA) for 1 h at 54 mA per blot. After transfer, membranes were placed in blocking solution [5% non-fat dry milk in Tris-buffered saline and 0.05% Tween<sup>®</sup> 20 (TBST)] for 1 h. Blots were either incubated with goat anti-GST primary antibody (1:1000 dilution, GE Healthcare, Piscataway, NJ) or with rabbit Anti-Active<sup>®</sup> (pTGpY) polyclonal IgG antibody (1:2000, Promega, Madison, WI) in TBST containing 1.0 mg/mL BSA and 0.01% sodium azide for 1 h. Membranes were then washed 3

times for 5 min with TBST and incubated for 1 h with alkaline phosphatase (AP)-linked secondary antibody. The secondary antibodies used were 1:5000 mouse anti-goat (Santa Cruz Biotechnology, Santa Cruz, CA) or 1:30,000 anti-rabbit (Sigma–Aldrich) when used in conjunction with the anti-GST primary antibody or the Anti-Active<sup>®</sup> p38 rabbit polyclonal IgG antibody, respectively. Bm-MPK1 was detected using 2.0 mL of Chromogenic Western Blue<sup>®</sup> Stabilized Substrate for AP (Promega).

### 2.5. p38 inhibitors

Human p38 inhibitors BIRB796 (Axon, Groningen, Netherlands), SB203580 (Selleck, Houston, TX) and RWJ67657 ([21] Dr. Fina Liotta, Montclair State University) were dissolved in 100% DMSO and stored at  $-20^\circ\text{C}$  prior to use.

### 2.6. Bm-MPK1 kinase assays

#### 2.6.1. [ $\gamma$ -<sup>32</sup>P] ATP assay

Bm-MPK1 protein kinase activity was assayed by monitoring the incorporation of <sup>32</sup>P from [ $\gamma$ -<sup>32</sup>P] ATP into myelin basic protein (MBP). Alternatively, Bm-MPK1 autophosphorylation was examined in the absence of MBP. Activated Bm-MPK1 (0.48  $\mu\text{M}$ ) was incubated with or without 1.0  $\mu\text{g}$  of MBP in 20  $\mu\text{L}$  containing 15 mM HEPES, (pH 7.4), 25 mM  $\beta$ -glycerophosphate, 15 mM NaCl, 10 mM  $\text{MgCl}_2$ , 1 mM EGTA, and 0.02% Tween<sup>®</sup> 20. Samples were pre-incubated for 10 min at 37 °C prior to adding the ATP (50  $\mu\text{M}$ , 0.4  $\mu\text{Ci}/\mu\text{L}$  [ $\gamma$ -<sup>32</sup>P] ATP). Following incubation at 37 °C for 20 min, reactions were terminated by adding NuPAGE<sup>®</sup> SDS sample buffer (Invitrogen) and subjected to SDS-PAGE as described above. Gels were stained, destained and dried onto blotting paper (Sigma) using a vacuum gel dryer prior to performing autoradiography using Kodak<sup>TM</sup> BioMax<sup>®</sup> Maximum Resolution film. Autoradiographs were analyzed using Image-J software [22].

#### 2.6.2. IMAP Bm-MPK1 kinase assay

Bm-MPK1 kinase activity was also assayed using the immobilized metal ion affinity-based fluorescence polarization (IMAP, Molecular Devices, Silicon Valley, CA) assay according to the manufacturer's instructions, in the presence of 100  $\mu\text{M}$  ATP, 1.0 mM DTT and where indicated, MKK6 (Sigma–Aldrich) and Bm-MPK1 (un-activated or activated) in reaction buffer – Tween-20 [10 mM Tris-HCl, pH 7.2, 10 mM  $\text{MgCl}_2$ , 0.05%  $\text{NaN}_3$ , and 0.01% Tween<sup>®</sup> 20 (RB-T), Molecular Devices]. Reactions were initiated with addition of 100–200 nM fluorescent substrate (FAM-p38tide, Molecular Devices), prepared in RB-T buffer. The fluorescent polarization was read in parallel and perpendicular with an excitation wavelength of 485 nm and an emission wavelength of 528 nm using a Synergy 2 Microplate reader (BioTek, Winooski, VT). Dose–response inhibitor assays were conducted as described above using 160 ng/well of sodium arsenate-activated Bm-MPK1 or 50 ng/well of commercial p38 $\alpha$  (Millipore, Temecula, CA). The data was analyzed using four parameter logistic curve using Microsoft Excel Solver and dose response curves were generated using Microsoft Excel.

### 2.7. *B. malayi* culture, p38 inhibitor treatment and phenotypic analysis

#### 2.7.1. Parasite motility

Female adult *B. malayi* parasites, harvested from infected jirds, were procured from the NIAID/NIH Filariasis Research Reagent Resource Center (FR3). Adult worms were plated in 24-well plates with 2 mL of Advanced RPMI 1640 medium (Invitrogen) supplemented with 25 mM HEPES, 2 mM L-Glutamine (Invitrogen), 100 U/mL Penicillin (Invitrogen), 100  $\mu\text{g}/\text{mL}$  Streptomycin (Invitrogen), 2.5  $\mu\text{g}/\text{mL}$  Amphotericin B solution (Invitrogen), and 5% heat



inactivated fetal bovine serum and placed in a 37 °C humidified incubator with 5% CO<sub>2</sub>. After 24 h, adult worms were selected based upon microfilariae release. Microfilariae release was scored as follows: (–) no microfilariae, (±) some microfilariae, (+) moderate levels of microfilariae, (++) and (+++) if the parasite secretes large quantities of microfilariae. After the parasites were scored, 6–9 worms were selected for each treatment group based on microfilariae release and were transferred to new plates. The microfilariae released in the old plate were pooled together, briefly centrifuged at 5000 × g for 5 min, and re-suspended in 2 mL of media. Microfilarial density was determined using a hemocytometer and plated in a 96-well plate, 80 microfilariae/well with 200 µL of complete media. Treatment groups received the p38 inhibitor, BIRB796 (1 µM or 10 µM), 5 mM sodium arsenate with 1 µM or 10 µM BIRB796, 0.1% DMSO (control) or 5 mM sodium arsenate vehicle control. Cultures were placed in a 37 °C humidified incubator with 5% CO<sub>2</sub>. The worms were transferred into a new plate containing fresh media and drug every 48 h. Parasite and microfilariae motility were given a score from 0 to 4 with 4, rapid movement and largely coiled; 3, moderated movement and uncoiled; 2, slow movement and uncoiled; 1, twitching movement and uncoiled; 0, no motility (dead). The motility of the worms and microfilariae were observed every 24 h and analyzed by a one sided unpaired Student's *t*-test using Microsoft Excel. All experiments were performed 2–3 times with similar results.

### 2.7.2. MTT viability assay

Viability was also assessed colorimetrically using 3-(4,5-dimethylthiazol-2-yl)-2,5-diphenyltetrazolium bromide (MTT). The assay was performed as described previously [23] with minor modifications. Briefly, worms were individually placed into a 96-well plate containing 180 µL of PBS, then 20 µL of a MTT solution (5 mg/mL in PBS) was added and the plate incubated at 37 °C for 30 min. All the solution was removed from the wells and 200 µL of DMSO was then added to the plate. The plate was incubated at 37 °C for 15 min and then placed on a shaker at room temperature for another 15 min. The absorbance of each sample was measured at 550 nm.

## 3. Results

### 3.1. Enzymatic activity of recombinant Bm-MPK1 using a fluorescently labeled substrate

Bm-MPK1 was successfully expressed as a GST-tagged protein in human HEK 293F cells. As mentioned previously, p38 MAPKs require activation by dual-phosphorylation of the TGY motif by upstream kinases [15]. All isoforms of human p38 MAP kinase have been shown to be activated by MKK6 [24]. Given the high degree of Bm-MPK1 sequence similarity to other p38 kinases and a conserved TGY motif (Fig. 1), we tested the ability of the upstream kinase activator of human p38, MKK6, to activate Bm-MPK1. Data obtained using the IMAP assay showed that Bm-MPK1 had very low kinase activity unless it was pre-incubated in the presence of active human MKK6 (Fig. 2A). Under the conditions of the assay, a concentration-dependent increase in Bm-MPK1 kinase activity was observed. The addition of the potent p38 kinase inhibitor, RWJ67657 [21] to the assay resulted in virtually complete inhibition of kinase activity (Fig. 2A). We further tested whether Bm-MPK1 could be activated by subjecting HEK 293F cells to sodium arsenate-induced oxidative stress, which generates reactive oxygen species. Mammalian proteins comprising the p38 pathway have been shown to be effectively activated using this approach [20]. Sodium arsenate-induced oxidative stress led to a dramatic activation of Bm-MPK1 (Fig. 2B). The addition of recombinant MKK6 to the reaction pro-

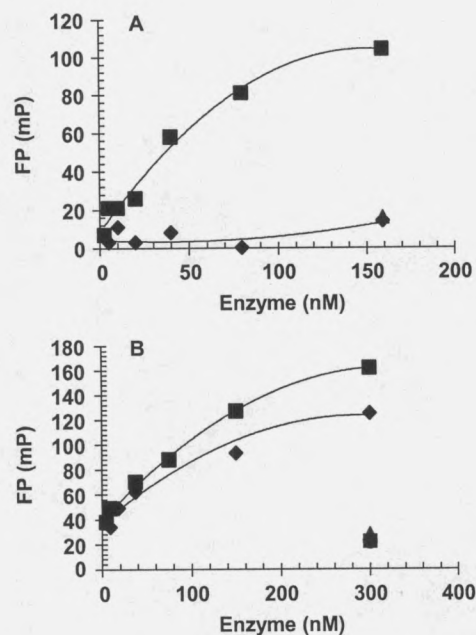


**Fig. 2.** IMAP Fluorescence Polarization assay of untreated and sodium arsenate-activated Bm-MPK1. The fluorescence polarization response is given as mP and is a measure of the change in substrate polarization due to phosphorylation. (A) Activation of Bm-MPK1 purified from Bm-MPK1/pDEST<sup>TM</sup>27-transfected HEK 293-F cells by incubation in the presence (■) or absence (◆) of MKK6. (B) Bm-MPK1 purified from Bm-MPK1/pDEST<sup>TM</sup>27-transfected HEK 293-F cells treated with 400 µM sodium arsenate for 3 h prior to harvesting the cells. Sodium arsenate-activated Bm-MPK1 incubated in the presence (■) or absence (◆) of MKK6. In both (A) and (B), sodium arsenate-activated Bm-MPK1 treated with 10 µM p38 inhibitor RWJ67657 (●) or MKK6-activated Bm-MPK1 treated with 10 µM p38 inhibitor RWJ67657 (▲) is also shown. The data was corrected for the blank (buffer only).

vided an additional, small, increase in kinase activity indicating that arsenate-induced oxidative stress leads to effective activation of Bm-MPK1. As before, the addition of the human p38 inhibitor, RWJ67657, effectively inhibited kinase activity (Fig. 2(B)). These results illustrate the highly conserved nature of nematode and human p38 kinases both in terms of their mechanism of activation as well as susceptibility to inhibition.

We next examined whether activation of Bm-MPK1 by oxidative stress results in dual phosphorylation of the TGY activation loop using a polyclonal Anti-Active<sup>®</sup> p38 antibody that specifically reacts against pTGPY motif in human p38. Western blots of purified Bm-MPK1 from sodium arsenate stressed HEK 293F cells showed increased phosphorylation compared to unstressed cells (Fig. 3A). An anti-GST antibody showed equivalent amounts of a 67 kDa immunoreactive band in all lanes (Fig. 3B), confirming that oxidative stress enhances phosphorylation. Moreover, these results further attest to the highly conserved nature of the TGY motif between human and *B. malayi* p38 MAPKs.

### 3.2. Enzymatic activity of Bm-MPK1 using [ $\gamma$ -<sup>32</sup>P]ATP

The IMAP assay for p38 in the previous experiments utilizes a peptide substrate. We next determined the ability of Bm-MPK1 to phosphorylate a generic MAPK substrate, myelin basic protein (MBP) using [ $\gamma$ -<sup>32</sup>P]ATP. Bm-MPK1 was capable of efficiently phosphorylating the 20 kDa MBP protein (Fig. 4, lane 3). Also, Bm-MPK1 was found to be capable of autophosphorylation indicated by the appearance of a radioactive band with a molecular weight of 67 kDa (Fig. 4, lane 2). Auto-phosphorylation is a common property of a number of MAPKs.

The effects of two p38 inhibitors exhibiting two distinct inhibitory mechanisms, BIRB796 [25] and RWJ67657 [21], were

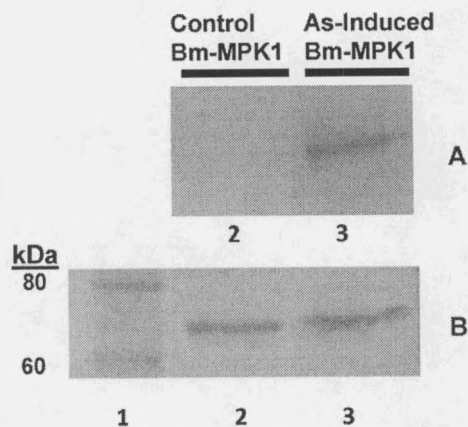


**Fig. 3.** Dual phosphorylation of the TGY motif in Bm-MPK1 by arsenate-induced oxidative stress. (A) Western blot developed with Anti-Active<sup>®</sup> p38 (pTGpY) rabbit polyclonal antibody. (B) Western blot developed with anti-GST goat antibody. Bm-MPK1 was expressed in HEK 293-F cells subjected to sodium arsenate-induced stress. Lane 1, Molecular weight markers; Lane 2, purified Bm-MPK1 (100 ng) from control cells; and Lane 3, purified Bm-MPK1 (100 ng) from sodium arsenate ( $\text{As} = \text{Na}_2\text{HAsO}_4$ )-stressed cells.

next examined. BIRB796 is a potent allosteric inhibitor active against all isoforms of human p38 [26]. RWJ67657 is a specific class of human p38 inhibitor that competes with ATP for the occupancy of the nucleotide binding domain of only p38 $\alpha$  and  $\beta$  isoforms [21]. Ten micromolar BIRB796 inhibited Bm-MPK1 activity by 94% while 10  $\mu\text{M}$  RWJ67657 only inhibited its activity by 61% (Fig. 5). The one micromolar BIRB796 inhibited Bm-MPK1 activity 73% while 1  $\mu\text{M}$  RWJ67657 inhibited Bm-MPK1 73%. In addition, both inhibitors inhibited Bm-MPK1 autophosphorylation (Fig. 5).

### 3.3. Comparison of p38 inhibitors dose responses for human p38 and Bm-MPK1

We next determined the relative potency of a small panel of p38 inhibitors against Bm-MPK1 and human p38 using the IMAP assay. To this end, dose response curves were generated for the ATP com-

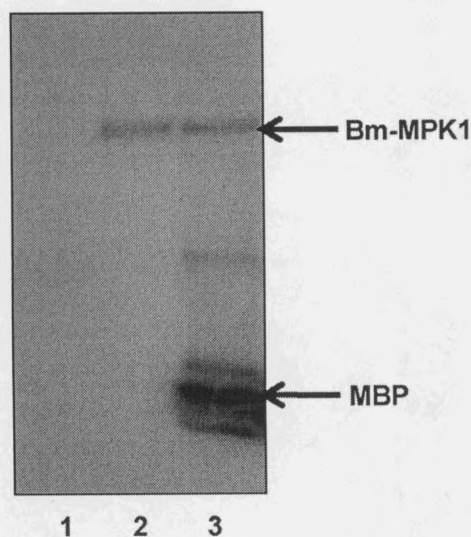


**Fig. 4.** Phosphorylation of Myelin Basic Protein (MBP) by Bm-MPK1. MBP was incubated with  $[\gamma\text{-}^{32}\text{P}]\text{ATP}$  in the absence and presence of Bm-MPK1 at 37 °C for 20 min. The reaction was terminated by the addition of SDS sample buffer and subjected to SDS-PAGE. Phosphorylation was detected by autoradiography. Lane 1,  $[\gamma\text{-}^{32}\text{P}]\text{ATP}$  and MBP; Lane 2,  $[\gamma\text{-}^{32}\text{P}]\text{ATP}$  and Bm-MPK1; and Lane 3,  $[\gamma\text{-}^{32}\text{P}]\text{ATP}$ , MBP, and Bm-MPK1.

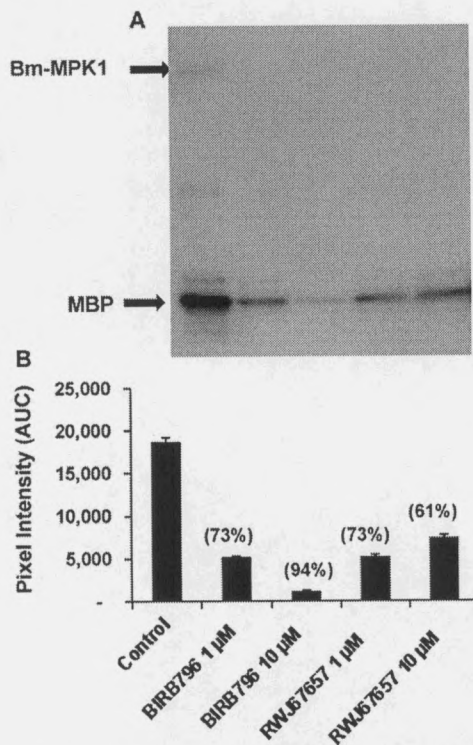


**Fig. 5.** Inhibition of Bm-MPK1 with p38 inhibitors BIRB796 and RWJ67657. Myelin Basic Protein (MBP) was incubated with  $[\gamma\text{-}^{32}\text{P}]\text{ATP}$  in the absence and presence of Bm-MPK1 at 37 °C for 20 min. The reaction was terminated by the addition of SDS sample buffer and the reaction mixture was subjected to SDS-PAGE. (A) Phosphorylation was detected by autoradiography. (B) Bands from (A) were scanned using ImageJ program and the area under the curve (AUC) calculated from pixel intensity. Lane 1, control, no inhibitor; Lane 2, 1  $\mu\text{M}$  BIRB796; Lane 3, 10  $\mu\text{M}$  BIRB796; Lane 4, 1  $\mu\text{M}$  RWJ67657; and Lane 5, 10  $\mu\text{M}$  RWJ67657. The percent inhibition was calculated based on control and is indicated in parenthesis. The gel was scanned using Image J three times. The bars represent mean  $\pm$  SD.

petitive p38 inhibitors, SB203580 [27] and RWJ67657 and for the allosteric inhibitor BIRB796. The relative potency of these inhibitors was assessed by determining the half maximal inhibitory concentration ( $\text{IC}_{50}$ ) for each inhibitor. SB203580, RWJ67657 and BIRB796 exhibited  $\text{IC}_{50}$  values of 218, 121 and 141 nM, respectively, against Bm-MPK1. The inhibitors each had much greater potency against human p38, having  $\text{IC}_{50}$  values of 33.5, 4.5 and 35.4 nM, respectively (Fig. 6 and Table 1), suggesting the existence of differences in the architecture of the inhibitor binding sites between the MAPKs. Nonetheless, these compounds are well within the sub-micromolar range for inhibition making them very attractive precursors for the development of more potent and selective Bm-MPK1 inhibitors.

### 3.4. Effects of p38 inhibitors on *B. malayi* stress responses

It is well documented that filarial parasites are highly resistant to oxidative stress [9,10], therefore we tested whether Bm-MPK1

**Table 1**  
Comparison of relative potency of p38 inhibitors against p38 and Bm-MPK1.

Compound	$\text{IC}_{50}$ (nM)		Ratio
	p38	Bm-MPK1	
SB203580	33.5 $\pm$ 10.6 (5)	218 $\pm$ 54.8 (4)	6
RWJ67657	4.5 $\pm$ 2.1 (2)	121 $\pm$ 1.5 (2)	36
BIRB796	35.4 $\pm$ 14.0 (4)	141 $\pm$ 44.7 (4)	4

The data is represented as mean of  $\text{IC}_{50}$  from separate experiments (count)  $\pm$  standard error.

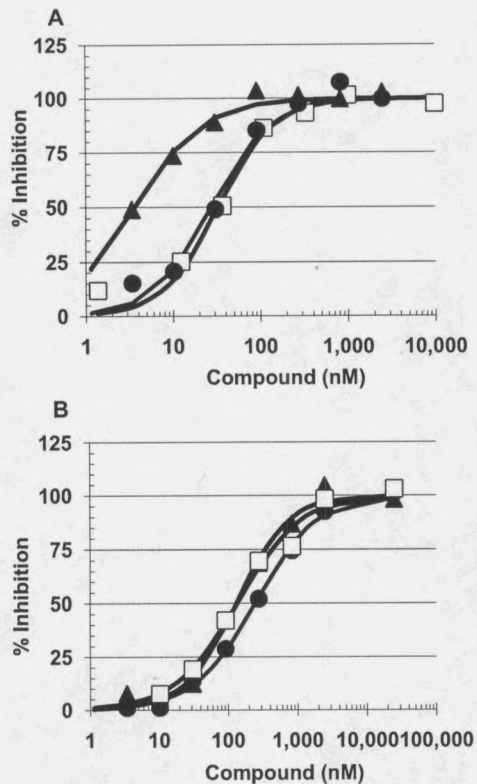


**Fig. 6.** Human p38 inhibitor dose–response analysis for p38 and Bm-MPK1. (A) Inhibition of human p38 activity by SB203580 (●), RWJ67657 (▲), or BIRB796 (□). (B) Inhibition of Bm-MPK1 activity by SB203580 (●), RWJ67657 (▲), or BIRB796 (□).

plays a role in protecting *B. malayi* from oxidative stress using BIRB796. This particular human p38 inhibitor was selected because of its potency and high selectivity against all human p38 isoforms [25,26]. In preliminary experiments we determined that BIRB796 exhibited pronounced effects on parasite motility, an established measure of parasite viability [28], at drug concentrations exceeding 10  $\mu$ M (data not shown). The relevance of direct effects of BIRB796 on *B. malayi* motility is unclear. The lack of a defined dose–response may indicate off target effects at high drug concentrations. Drug uptake and distribution in parasitic nematodes is complex and not well defined [29] and the actual concentration of BIRB796 within the parasite is unknown. Upon establishing a concentration of BIRB796 that did not affect motility, we determined whether the combination of 10  $\mu$ M BIRB796 and 5 mM sodium arsenate affected *B. malayi* motility. Similar to *C. elegans*, *B. malayi* are largely resistant to oxidative stress induced with 5 mM sodium arsenate ([12] and Fig. 7). Interestingly, the combination of 10  $\mu$ M BIRB796 and 5 mM sodium arsenate resulted in a dramatic decrease in parasite motility by 88% compared to control (Fig. 7). Additionally, *B. malayi* parasites were also subjected to an MTT assay to determine whether the viability of the parasites on day 6 would correspond to the observed decrease in motility. Addition of 10  $\mu$ M BIRB796 and 5 mM sodium arsenate reduced the viability of the parasite by >84%, confirming the relationship between parasite motility and viability (Fig. 8). These results support the notion that Bm-MPK1, like the *C. elegans* ortholog PMK-1, plays a role in protecting *B. malayi* from toxic oxidative stress.

We next examined the effects of BIRB796 on the ability of microfilariae to respond to oxidative stress induced by sodium arsenate. Microfilariae are significantly more sensitive to arsenate-induced oxidative stress than adult worms (Fig. 9). This is consistent with observations made by others where microfilariae were shown to

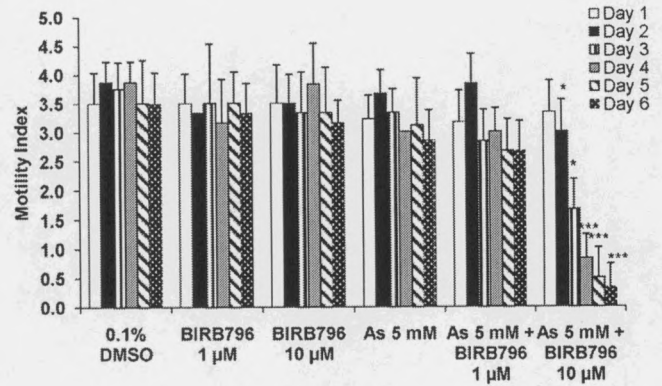


**Fig. 7.** Effects of sodium arsenate-induced oxidative stress on adult *B. malayi* motility in the presence or absence of BIRB796. Female worms were cultured with 0.1% DMSO (control), 1  $\mu$ M BIRB796, 10  $\mu$ M BIRB796, 5 mM sodium arsenate alone, 5 mM sodium arsenate with 1  $\mu$ M BIRB796 and 5 mM sodium arsenate with 10  $\mu$ M BIRB796 for 6 days. Parasite motility was observed every 24 h and a score 0–4 was given: \* $p$  < 0.01, \*\*\* $p$  < 0.0001 by a one-tailed unpaired Student's *t*-test using sodium arsenate as a vehicle control for sodium arsenate with BIRB796 and 0.1% DMSO as a vehicle control for BIRB796 and sodium arsenate alone.  $n$  = 5 or 6 worms. Bars represent mean  $\pm$  SD.

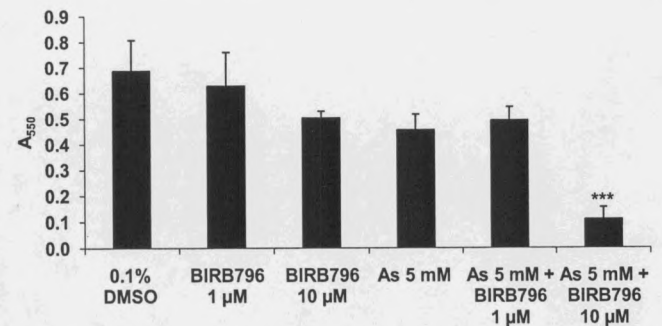


**Fig. 8.** Effects of BIRB796 on adult *B. malayi* responses to arsenate-induced oxidative stress as assessed by MTT assay on day 6. Female adult worms were cultured with 0.1% DMSO (control), 1  $\mu$ M and 10  $\mu$ M BIRB796, 5 mM sodium arsenate and 5 mM sodium arsenate with 1  $\mu$ M or 10  $\mu$ M BIRB796 for 6 days: \*\*\* $p$  < 0.0001 by a one-tailed unpaired Student's *t*-test using sodium arsenate as a vehicle control for sodium arsenate with 1  $\mu$ M or 10  $\mu$ M BIRB796 and 0.1% DMSO as a vehicle control for BIRB796 and sodium arsenate alone.  $n$  = 2–9 worms. Bars represent mean  $\pm$  SD.

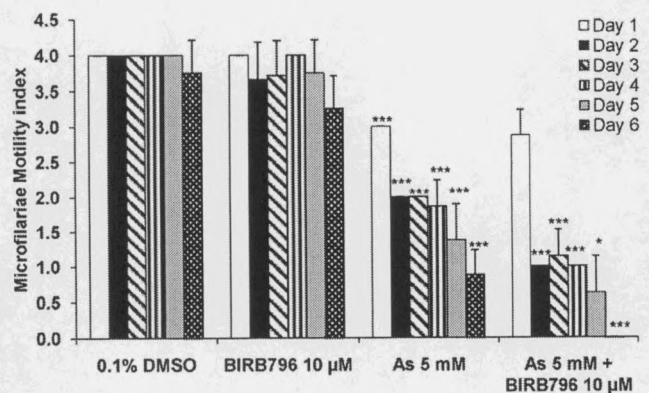


**Fig. 9.** Effects of BIRB796 on *B. malayi* microfilariae motility under sodium arsenate-induced oxidative stress. Microfilariae (80 microfilariae/well) were cultured with 0.1% DMSO (control), 10  $\mu$ M BIRB796, 5 mM sodium arsenate, and 5 mM sodium arsenate with 10  $\mu$ M BIRB796 for 6 days in a 96-well plate. The motility of the microfilariae were observed every 24 h and a score 0–4 was given: \* $p$  < 0.01, \*\*\* $p$  < 0.0001 by a one sided unpaired Student's *t*-test using sodium arsenate as a vehicle control for sodium arsenate with 10  $\mu$ M BIRB796 and 0.1% DMSO as a vehicle control for BIRB796 and sodium arsenate alone.  $n$  = 6 wells. Bars represent mean  $\pm$  SD.

be more sensitive to oxidative stress induced with hydrogen peroxide [11]. Over the course of 6 days, a significant reduction in microfilarial motility was observed in the presence of 5 mM sodium arsenate. Addition of 10  $\mu$ M BIRB796 resulted in a statistically significant reduction in motility over what was observed with treatment with sodium arsenate alone (Fig. 9). These results indicate that, Bm-MPK1 plays a role in microfilarial responses to ROS.

#### 4. Discussion

This paper describes the biochemical characterization of a *B. malayi* stress-activated p38/PMK-1 kinase ortholog Bm-MPK1 along with an analysis of the effects of p38 inhibitors on Bm-MPK1 kinase activity and on the ability of *B. malayi* to respond to ROS. Bm-MPK1 is highly homologous to *C. elegans* PMK-1 which is known to play a critical role in protection against oxidative stress and innate immunity [12–14]. Genetic deletion of PMK-1, or its upstream activator SEK-1, attenuates *C. elegans* responses to oxidative stress induced by sodium arsenate [12]. Tissue dwelling filarial parasites such as the lymphatic parasites *W. bancrofti* and *B. malayi* and cutaneous *O. volvulus* strongly modulate host immune responses through several mechanisms [7–9]. These organisms tend to be long lived in their hosts and as such, must deal with host immune responses to avoid elimination while sparing the host from severe, life threatening pathology. An early first line of defense against parasitic infection is the generation of reactive oxygen and nitrogen species (RNS) by macrophages and granulocytes [30]. ROS represents a class of highly reactive chemical species such as superoxide anion ( $O_2^-$ ) that are formed in these cells through the action of NADPH oxidase [31]. *B. malayi*, like other parasites, produces several secreted and non-secreted enzymes such as superoxide dismutase (SOD), thioredoxin peroxidase and glutathione peroxidase for defense against oxidative damage [30].

The biochemistry of nematode anti-oxidation mechanisms has been extensively studied in the free-living nematode, *C. elegans*. It has been shown in *C. elegans* that a mitogen-activated protein kinase pathway (MAPK) is critically important for regulating responses to oxidative stress as well as xenobiotic detoxification and innate immunity [12,13]. In response to oxidative stress, *C. elegans* PMK-1 kinase, an ortholog of human p38 kinase, is activated and directly phosphorylates SKN-1, a transcription factor important for embryonic mesodermal development and regulation of oxidative stress responses in the adult [16]. Phosphorylation of SKN-1 by PMK-1 results in the translocation of SKN-1 into intestinal nuclei where it functions in the regulation of the expression of a variety of antioxidant and phase II detoxification genes such as SOD [16]. Regulation of SKN-1 transcriptional activity through phosphorylation is likely to be more complex since, in addition to PMK-1, it is a substrate for at least four additional protein kinases [32]. Unlike *C. elegans*, little is known regarding the biochemical and molecular details of the regulation of anti-oxidative responses in parasitic nematodes. In the study presented here, we have characterized a PMK-1/p38 ortholog, Bm-MPK1, from the human filarial parasite, *B. malayi*. Using a chemical biological approach, we have demonstrated inhibition of Bm-MPK1 activity with known ATP competitive and allosteric p38 inhibitors. Furthermore, we have demonstrated that the potent allosteric p38 inhibitor, BIRB796, suppresses *B. malayi* anti-oxidative responses to ROS induced by sodium arsenate. We have also shown that treatment of adult female worms with BIRB796, under oxidative stress conditions, results in death of the parasites. Additional studies are underway to determine the effects of BIRB796 on stress responses in other developmental stages of *B. malayi*, especially L3 larvae, the infectious larval form of *B. malayi* introduced into the host from a mosquito vector.

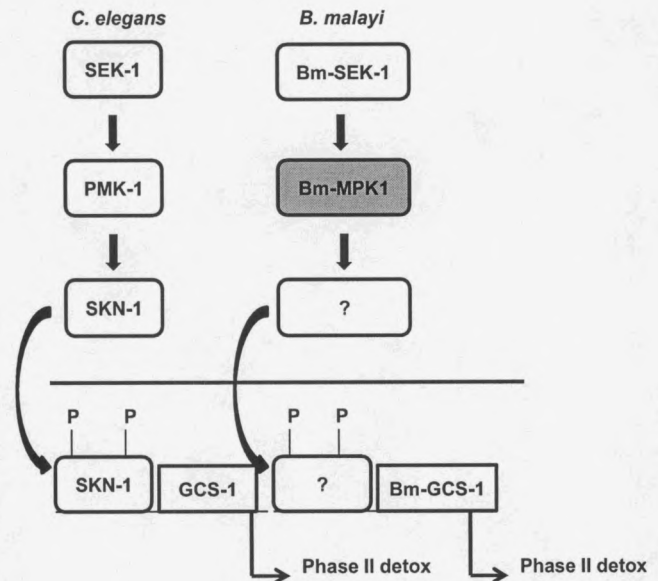


Fig. 10. Comparison of *B. malayi* Bm-MPK1 and *C. elegans* PMK-1 stress-activated signaling pathways.

The *B. malayi* Bm-MPK1 pathway shares several similarities to the *C. elegans* PMK-1 pathway (Fig. 10) including the presence of orthologs of upstream activating protein kinases such as SEK-1 [5]. However, there are also differences such as the apparent absence of an SKN-1 ortholog in *B. malayi* [33]. Additional studies are underway in our laboratory to further define this pathway. One important aspect of this work is the use of chemical probes to study parasitic nematode signaling pathways. Unlike *C. elegans* and protozoal parasites, filarial parasites are frequently resistant to manipulation using standard molecular genetics approaches such as RNAi [34,35]. Synthetic inhibitors, therefore, provide an alternative, chemical biological, approach to study gene function in these organisms. Our results, in addition to defining the biochemical mechanisms involved in parasitic nematode responses to oxidative stress, may offer a potential strategy for treating filarial disease. The design of highly selective and potent Bm-MPK1 inhibitors could potentially be used to interfere with Bm-MPK1 induction of drug detoxification genes such as gamma-glutamylcysteine synthetase (*gcs-1*) which catalyzes the first, rate-limiting step in the biosynthesis of glutathione (GSH). *C. elegans* (*GCS-1*), is known to be regulated through the PMK-1/SKN-1 pathway and plays a role in resistance to oxidative stress in this organism [12]. Mentioned earlier, GSH, along with GST, glutathione peroxidase (GP) and glutathione reductase (GR), constitute an important antioxidant system in filarial parasites contributing to their long-term survival in the host [30]. Filarial parasite GST has been targeted for the development of anti-parasitic drugs [36,37]. Disruption of this pathway with Bm-MPK1 inhibitors may compromise the ability of filarial parasites to counteract host oxidative stress responses. In addition, the potential detoxification of known anti-filarial drugs by conjugation with reduced glutathione through the action of GST may be attenuated allowing for an increase in potency and efficacy of known anti-parasitic drugs. In conclusion, we have demonstrated, through a chemical biological approach, that the *B. malayi* stress-activated MAPK, Bm-MPK1, functions in a signaling pathway important for parasite anti-oxidative responses to ROS. The presence of highly homologous Bm-MPK1 orthologs in other filarial and non-filarial parasites indicates a similar role for these kinases in anti-oxidative and detoxification processes. Further characterization of this pathway will provide additional insights into filarial parasite responses

to host-generated ROS and the therapeutic potential of inhibiting this response.

### Acknowledgements

We gratefully acknowledge Dr. Sara Lustigman of the New York Blood Center (New York, NY), for her help and expert advice in working with *B. malayi* parasites and Dr. Fina Liotta of Rutgers University (Newark, NJ) for synthesis of RWJ67657. We also thank the NIAID/NIH Filariasis Research Reagent Resource Center (FR3) for providing parasites used in these studies. This work is supported by The Herman and Margret Sokol Endowment at Montclair State University.

### References

- [1] Singh PK, Ajay A, Kushwaha S, et al. Towards novel antifilarial drugs: challenges and recent developments. *Future Med Chem* 2010;2:251–83.
- [2] Bockarie MJ, Taylor MJ, Gyapong JO. Current practices in the management of lymphatic filariasis. *Expert Rev Anti-Infect Ther* 2009;7:595–605.
- [3] Geary TG, Woo K, McCarthy JS, et al. Unresolved issues in anti-helminthic pharmacology for helminthiasis of humans. *Int J Parasitol* 2010;40:1–13.
- [4] Lustigman S, McCarter JP. Ivermectin resistance in *Onchocerca volvulus*: toward a genetic basis. *PLoS Negl Trop Dis* 2007;1:1–3.
- [5] Ghedin E, Wang S, Spiro D, et al. Draft genome of the filarial nematode parasite *Brugia malayi*. *Science* 2007;317:1756–60.
- [6] Robinson MW, Hutchinson AT, Dalton JP, Donnelly S. Peroxiredoxin: a central player in immune modulation. *Parasit Immun* 2010;32:305–13.
- [7] Sorci G, Faivre B. Inflammation and oxidative stress in vertebrate host–parasite systems. *Phil Trans R Soc B* 2009;364:71–83.
- [8] Maizels RM, Yazdanbakhsh M. Immune regulation by helminth parasites: cellular and molecular mechanisms. *Nat Rev Immun* 2003;3:733–44.
- [9] Maizels RM, Blaxter ML, Scott AL. Immunological genomics of *Brugia malayi*: filarial genes implicated in immune evasion and protective immunity. *Parasit Immun* 2001;23:327–44.
- [10] Awasthi SK, Mishra N, Dixit SK, et al. Antifilarial activity of 1,3-diarylpropenone: effect on glutathione-S-transferase, a phase II detoxification enzyme. *Am J Trop Med Hyg* 2009;80:764–8.
- [11] Selkirk ME, Smith VP, Thomas R, Gounaris K. Resistance of filarial nematode parasites to oxidative stress. *Int J Parasitol* 1998;28:1315–32.
- [12] Inoue H, Hisamoto N, An JH, et al. The *C. elegans* p38 MAPK pathway regulates nuclear localization of the transcription factor SKN-1 in oxidative stress response. *Genes Dev* 2005;19:2278–83.
- [13] An JH, Vranas K, Lucke M, et al. Regulation of the *Caenorhabditis elegans* oxidative stress defense protein SKN-1 by glycogen synthase kinase-3. *Proc Natl Acad Sci USA* 2005;102:16275–80.
- [14] Troemel ER, Chu SW, Reinke V, Lee SS, Ausubel FM, Kim DH. p38 MAPK regulates expression of immune response genes and contributes to longevity in *C. elegans*. *PLoS Genet* 2006;2:1725–39.
- [15] Coulthard L, White D, Jones D, McDermott M, Burchill S. p38 MAPK: stress responses from molecular mechanisms to therapeutics. *Trends Mol Med* 2009;15:369–79.
- [16] An JH, Blackwell TK. SKN-1 links *C. elegans* mesendodermal specification to a conserved oxidative stress response. *Genes Dev* 2003;17:1882–93.
- [17] Liotta F, Siekierka JJ. Apicomplexa, trypanosome and parasitic nematode protein kinases as antiparasitic therapeutic targets. *Curr Opin Invest Drugs* 2010;11:147–56.
- [18] Labarca C, Paigen K. A simple, rapid, and sensitive DNA assay procedure. *Anal Biochem* 1980;102:344–52.
- [19] Strober W. Trypan Blue exclusion test of cell viability. *Curr Proto Immunol* 2001:3B.
- [20] Zaho Q, Chen P, Manson ME, Liu Y. Production of active recombinant mitogen-activated protein kinases through transient transfection of 293T cells. *Prot Exp Purif* 2006;46:468–74.
- [21] Wadsworth SA, Cavender DE, Beers SA, et al. RWJ 67657, a potent, orally active inhibitor of p38 mitogen-activated protein kinase. *J Pharmacol Exp Ther* 1999;291:680–7.
- [22] Collins TJ. ImageJ for microscopy. *Biotechniques* 2007;43:25–30.
- [23] Comley JCW, Rees MJ, Turner CH, Jenkins DC. Colorimetric quantitation of filarial viability. *Int J Parasitol* 1989;19:77–83.
- [24] Keesler GA, Bray J, Hunt J, et al. Purification and activation of recombinant p38 isoforms  $\alpha$ ,  $\beta$ ,  $\gamma$ , and  $\delta$ . *Prot Exp Purif* 1998;14:221–8.
- [25] Pargellis C, Tong L, Churchill L, et al. Inhibition of p38 MAP kinase by utilizing a novel allosteric binding site. *Nat Struct Biol* 2002;9:268–72.
- [26] Kuma Y, Sabio G, Bain J, Shpiro N, Marquez R, Cuenda A. BIRB796 inhibits all p38 MAPK isoforms *in vitro* and *in vivo*. *J Biol Chem* 2005;280:19472–9.
- [27] Cuenda A, Rouse J, Doza YN, et al. SB 203580 is a specific inhibitor of a MAP kinase homolog which is stimulated by cellular stresses and interleukin 1. *FEBS Lett* 1995;364:229–33.
- [28] Comley JCW, Townson S, Rees MJ, Dobinson A. The further application of MTT-formazan colorimetry to studies on filarial worm viability. *Trop Med Parasitol* 1989;40:311–6.
- [29] Alvarez LI, Mottier ML, Lanusse CE. Drug transfer into target helminth parasites. *Trends Parasitol* 2007;23:98–104.
- [30] Chiumiento L, Bruschi F. Enzymatic antioxidant systems in helminth parasites. *Parasitol Res* 2009;105:593–603.
- [31] Bokoch GM. NADPH oxidases in innate immunity. *J Innate Imm* 2009;1:507–8.
- [32] Kell A, Ventura N, Kahn N, Johnson TE. Activation of SKN-1 by novel kinases in *Caenorhabditis elegans*. *Free Radic Biol Med* 2007;43:1560–6.
- [33] Maduro MF. Endomesoderm specification in *Caenorhabditis elegans* and other nematodes. *BioEssays* 2006;28:1010–22.
- [34] Geldhof P, Visser A, Clark D, et al. RNA interference in parasitic helminths: current situation, potential pitfalls and future prospects. *Parasitology* 2007;134:609–19.
- [35] Knox DP, Geldhof P, Visser A, Britton C. RNA interference in parasitic nematodes of animals: a reality check? *Trends Parasitol* 2007;23:105–7.
- [36] Yadav M, Singh A, Rathaur S, Liebau E. Structural modeling and simulation studies of *Brugia malayi* glutathione-S-transferase with compounds exhibiting antifilarial activity: implications in drug targeting and designing. *J Mol Graph Model* 2010;28:435–45.
- [37] Rao UR, Salinas G, Mehta K, Klei TR. Identification and localization of glutathione S-transferase as a potential target enzyme in *Brugia* species. *Parasitol Res* 2000;86:908–15.